Supporting Information: Vapor- and liquid-phase adsorption of alcohol and water in silicalite-1 synthesized in fluoride media

Robert F. DeJaco,[†,‡,⊥] Matheus Dorneles de Mello,[†,⊥] Huong Giang T. Nguyen,[¶] Mi Young Jeon,[†] Roger D. van Zee,[¶] Michael Tsapatsis,[*,†,§,‖] and J. Ilja Siepmann[*,†,‡]

†*Department of Chemical Engineering and Materials Science, University of Minnesota, 412 Washington Avenue SE, Minneapolis, Minnesota 55455-0132, United States*

‡*Department of Chemistry and Chemical Theory Center, University of Minnesota, 207 Pleasant Street SE, Minneapolis, Minnesota, 55455-0431, United States*

¶*Facility for Adsorbent Characterization and Testing, Material Measurement Laboratory, National Institute of Standards and Technology, Gaithersburg, Maryland 20899, United States*

§*Department of Chemical and Biomolecular Engineering, Johns Hopkins University, 3400 North Charles Street, Baltimore, Maryland 21218, United States*

‖*Department of Research and Exploratory Development, Applied Physics Laboratory, Johns Hopkins University, 11100 Johns Hopkins Road, Laurel, Maryland 20723-6099*

⊥*Contributed equally to this work*

E-mail: tsapatsis@jhu.edu; siepmann@umn.edu

Contents

S1 Supplementary Methods

S1.1 Coadsorption Relations

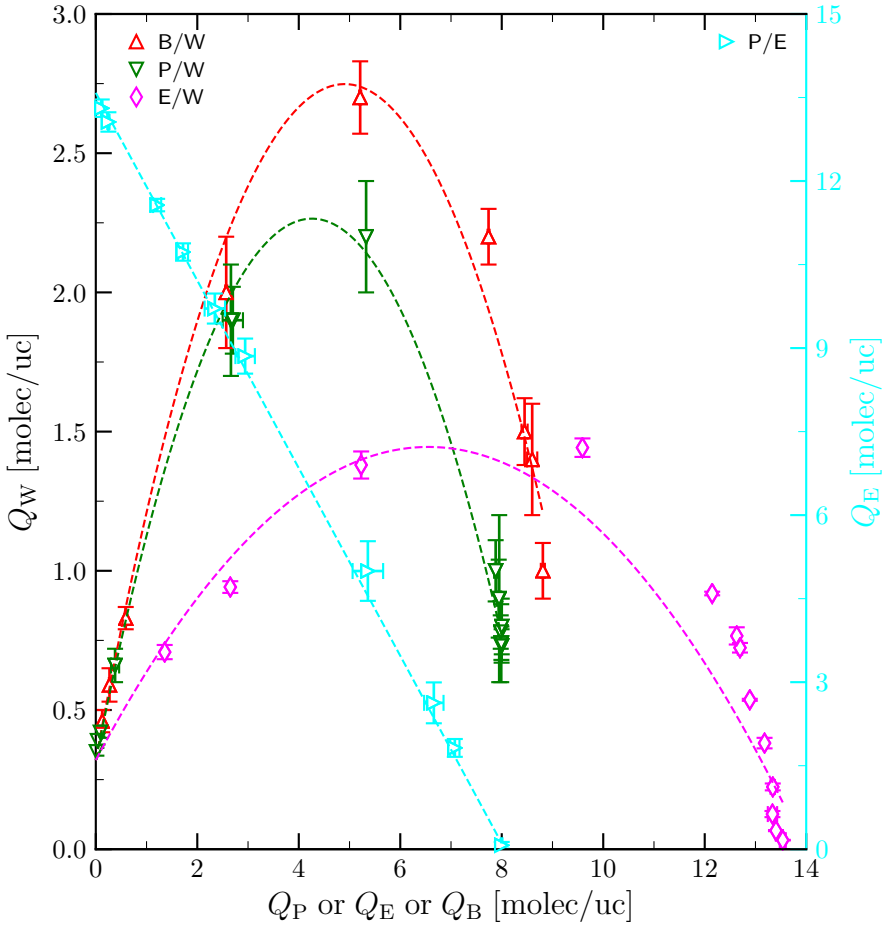

Figure S1: (left y-axis) Loading of water (Q_W) as a function of alcohol loading (Q_E or Q_B or Q_P) obtained by molecular simulations at $T = 323$ K and $p = 1.0$ bar for butane-1,4-diol/water mixtures (B/W), pentane-1,5-diol/water mixtures (P/W) or ethanol/water mixtures (E/W). (Right y-axis, cyan) Loading of ethanol (Q_E) as a function of pentane-1,5-diol loading for pentane-1,5-diol/ethanol mixtures (P/E) obtained by molecular simulations at the same temperature and pressure. Dashed lines are second-order polynomial fits to points of the same color, and are utilized in the coadsorption approach for calculation of experimental isotherms. The coefficients of each polynomial are reported in Table S1.

Table S1: Polynomial Coefficients for Coadsorption Model[a]

System	P/W	B/W	E/W	P/E
a_2	-0.1072 ± 0.0060	-0.1009 ± 0.0051	-0.02618 ± 0.00051	0
a_1	0.913 ± 0.048	0.990 ± 0.042	0.3433 ± 0.0066	-1.685 ± 0.013
a_0	0.320 ± 0.032	0.320 ± 0.032	0.320 ± 0.032	13.584 ± 0.078

[a] The units of coefficient a_k is $\frac{\text{molec solvent}}{\text{unit cell}} \left(\frac{\text{unit cell}}{\text{molec diol}}\right)^k$

S1.2 Solution Density Relations

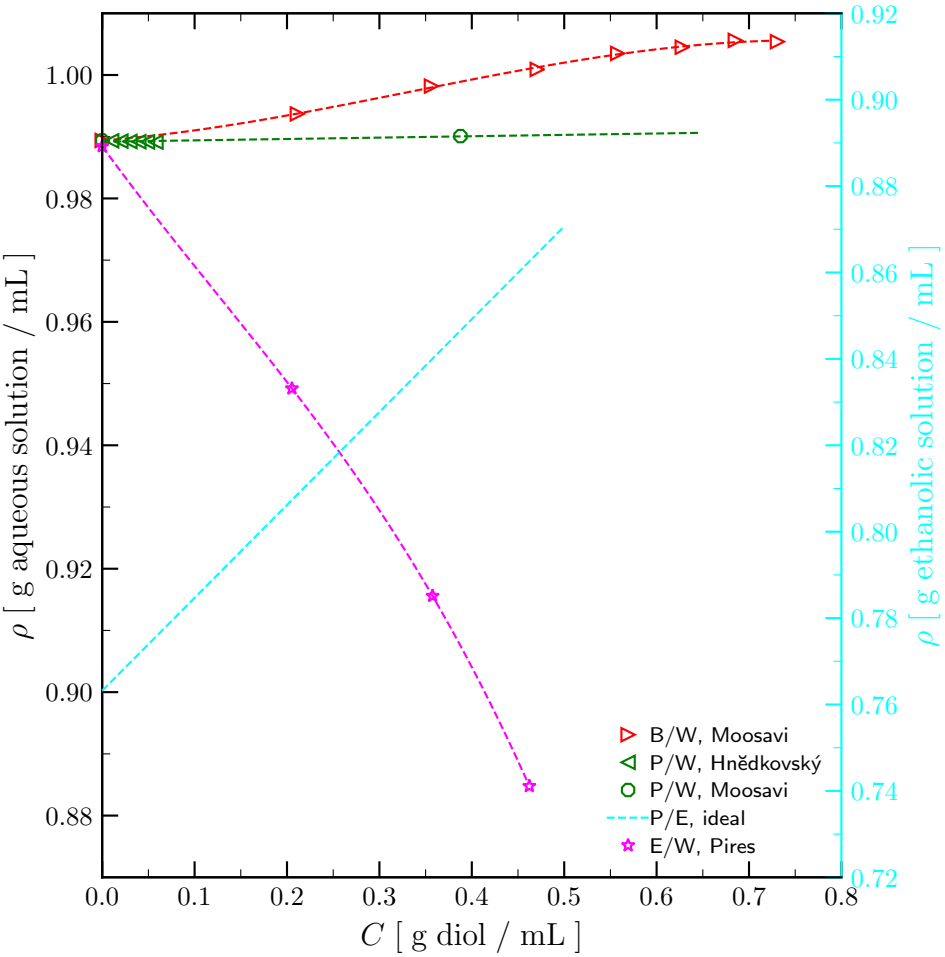

Figure S2: Aqueous solution densities (left y-axis) as a function of alcohol solution concentration fit to experimental measurements[S1–S3] at $T = 313$ and 318 K after extrapolation to 323 K. Ethanolic solution densities (right y-axis, cyan) as a function of diol solution concentrations obtained at $T = 323$ K by assuming ideal solution and using pure component densities from literature.[S2,S3] The dashed lines depict the functions used in calculation of experimental loadings in this work.

S1.3 Expressions for Q_{S} and Q_{A}

The diol loading calculated by the XS approach is expressed as

$$Q_{\mathrm{A}}^{\mathrm{XS}} = \frac{V_{\mathrm{in}} \left(C_{\mathrm{A,in}} - C_{\mathrm{A,eq}} \right)}{m} \tag{1}$$

The solvent loading calculated by the XS approach is expressed as

$$Q_{\mathrm{S}}^{\mathrm{XS}} = \frac{V_{\mathrm{in}} \left[\rho_{\mathrm{in}} - \rho_{\mathrm{eq}} - \left(C_{\mathrm{A,in}} - C_{\mathrm{A,eq}} \right) \right]}{m} \tag{2}$$

The diol loading calculated by the NS approach is expressed as

$$Q_{\mathrm{A}}^{\mathrm{NS}} = \frac{V_{\mathrm{in}} \left[\rho_{\mathrm{in}} - \left(\frac{C_{\mathrm{A,in}}}{C_{\mathrm{A,eq}}} \rho_{\mathrm{eq}} \right) \right]}{m \left(1 - \frac{\rho_{\mathrm{eq}}}{C_{\mathrm{A,eq}}} \right)} \tag{3}$$

By definition, the solvent loading for the NS approach is zero. The diol loading calculated by the VC approach is expressed as

$$Q_{\mathrm{A}}^{\mathrm{VC}} = \frac{V_{\mathrm{in}} \left(C_{\mathrm{A,in}} - C_{\mathrm{A,eq}} \right)}{m \left(1 - \frac{C_{\mathrm{A,eq}}}{\rho_{\mathrm{A}}} \right)} \tag{4}$$

The solvent loading calculated by the VC approach is expressed as

$$Q_{\mathrm{S}}^{\mathrm{VC}} = \frac{V_{\mathrm{in}}}{m} \left[\rho_{\mathrm{in}} - \rho_{\mathrm{eq}} - \left(1 - \frac{\rho_{\mathrm{eq}}}{\rho_{\mathrm{A}}} \right) \left(\frac{C_{\mathrm{A,in}} - C_{\mathrm{A,eq}}}{1 - \frac{C_{\mathrm{A,eq}}}{\rho_{\mathrm{A}}}} \right) \right] \tag{5}$$

The diol loading calculated by the PF approach is expressed as

$$Q_{\mathrm{A}}^{\mathrm{PF}} = \frac{V_{\mathrm{in}} \left[\rho_{\mathrm{in}} - \left(\frac{C_{\mathrm{A,in}}}{C_{\mathrm{A,eq}}} \rho_{\mathrm{eq}} \right) \right] - m \rho_{\mathrm{S}} V_{\mathrm{p}}}{m \left(1 - \frac{\rho_{\mathrm{eq}}}{C_{\mathrm{A,eq}}} - \frac{\rho_{\mathrm{S}}}{\rho_{\mathrm{A}}} \right)} \tag{6}$$

The solvent loading calculated by the PF approach is expressed as

$$Q_{\mathrm{S}}^{\mathrm{PF}} = V_{\mathrm{p}}\rho_{\mathrm{S}} - \frac{\rho_{\mathrm{S}}}{\rho_{\mathrm{A}}}\left(\frac{V_{\mathrm{in}}\left[\rho_{\mathrm{in}} - \left(\frac{C_{\mathrm{A,in}}}{C_{\mathrm{A,eq}}}\rho_{\mathrm{eq}}\right)\right] - m\rho_{\mathrm{S}}V_{\mathrm{p}}}{m\left(1 - \frac{\rho_{\mathrm{eq}}}{C_{\mathrm{A,eq}}} - \frac{\rho_{\mathrm{S}}}{\rho_{\mathrm{A}}}\right)}\right) \tag{7}$$

In order to calculate the diol loading for the CA approach, Equations 1, 2, and 7 are combined to yield a quadratic polynomial in $Q_{\mathrm{A}}^{\mathrm{CA}}$. The only positive root of the polynomial allows for calculation of $Q_{\mathrm{A}}^{\mathrm{CA}}$ as

$$Q_{\mathrm{A}}^{\mathrm{CA}} = \frac{-m_{\mathrm{z}}\left(1 + a_1 - \frac{\rho_{\mathrm{eq}}}{C_{\mathrm{A,eq}}}\right) - \sqrt{m_{\mathrm{z}}^2\left(1 + a_1 - \frac{\rho_{\mathrm{eq}}}{C_{\mathrm{A,eq}}}\right)^2 + 4a_2m_{\mathrm{z}}\left(V_{\mathrm{in}}\rho_{\mathrm{in}} - a_0m_{\mathrm{z}} - \frac{C_{\mathrm{A,in}}V_{\mathrm{in}}\rho_{\mathrm{eq}}}{C_{\mathrm{A,eq}}}\right)}}{2a_2m_{\mathrm{z}}} \tag{8}$$

For the P/E mixture, since a suitable fit was obtained with $a_2 = 0$, the loading was instead calculated as

$$Q_{\mathrm{A,P/E}}^{\mathrm{CA}} = \frac{V_{\mathrm{in}}\rho_{\mathrm{in}} - a_0m_{\mathrm{z}} - \frac{C_{\mathrm{A,in}}V_{\mathrm{in}}\rho_{\mathrm{eq}}}{C_{\mathrm{A,eq}}}}{m_{\mathrm{z}}\left(1 + a_1 - \frac{\rho_{\mathrm{eq}}}{C_{\mathrm{A,eq}}}\right)} \tag{9}$$

The solvent loading for the CA approach was then determined from the coadsorption fit, as expressed as

$$Q_{\mathrm{S}}^{\mathrm{CA}} = \sum_{k=0}^{2} a_k \left(Q_{\mathrm{A}}^{\mathrm{CA}}\right)^k \tag{10}$$

where $\{a_k\}$ are the coefficients determined from simulation.

S1.4 Supplementary Conversion Factors and Parameters

The following conversion factor was used to convert the loading of each sorbate i from g / g to molec / uc

$$Q_i \text{ [molec/uc]} = Q_i \text{ [g/g]} \times \left(\frac{192 M_{\mathrm{O}} + 96 M_{\mathrm{Si}}}{M_i} \right) \tag{11}$$

where M_i is the molecular weight of sorbate i, M_{O} is the atomic mass of Oxygen, and M_{Si} is the atomic mass of Silicon.

Table S2: Parameters Investigated in Pore Filling Model

i	$Q_i^{\max}$ [molec/uc]	$\rho_{i,\mathrm{liquid}}$ [g/mL]	V_{p} [mL/g]
N			0.186 (Ref. S4)
W	40.4 (Refs. S4,S5)	0.9894 ($T = 323$ K, Ref. S6)	0.125
E	13.31 ± 0.16 (Simulation)	0.7660 ($T = 320$ K, Ref. S7)	0.139
B	8.81 ± 0.04 (Simulation)	1.0008 ($T = 318.15$ K, Ref. S2)	0.138
P	7.9997 ± 0.0002 (Simulation)	0.9748 ($T = 318.15$ K, Ref. S2)	0.148

S1.5 VC Solvent Loading for An Ideal Solution

The solvent loading for the volume-change-by-solute-adsorption (VC) method is calculated by Equation 5. The total density ρ before or after adsorption can be expressed as a function of solute concentration C_{A} for an ideal solution as

$$\rho = \rho_{\mathrm{S}} + C_{\mathrm{A}} \left(1 - \frac{\rho_{\mathrm{S}}}{\rho_{\mathrm{A}}}\right) \tag{12}$$

and substitution into Equation 5 yields

$$\begin{aligned}
Q_{\mathrm{S}}^{\mathrm{VC}} &= \frac{V_{\mathrm{in}}}{m} \left[(C_{\mathrm{A,in}} - C_{\mathrm{A,eq}}) \left(1 - \frac{\rho_{\mathrm{S}}}{\rho_{\mathrm{A}}}\right) - \left(1 - \frac{\rho_{\mathrm{S}} + C_{\mathrm{A,eq}} \left(1 - \frac{\rho_{\mathrm{S}}}{\rho_{\mathrm{A}}}\right)}{\rho_{\mathrm{A}}}\right) \left(\frac{C_{\mathrm{A,in}} - C_{\mathrm{A,eq}}}{1 - \frac{C_{\mathrm{A,eq}}}{\rho_{\mathrm{A}}}}\right) \right] \\
&= \frac{V_{\mathrm{in}}}{m} (C_{\mathrm{A,in}} - C_{\mathrm{A,eq}}) \left[1 - \frac{\rho_{\mathrm{S}}}{\rho_{\mathrm{A}}} - \left(\frac{\rho_{\mathrm{A}} - \rho_{\mathrm{S}} - C_{\mathrm{A,eq}} \left(\frac{\rho_{\mathrm{A}} - \rho_{\mathrm{S}}}{\rho_{\mathrm{A}}}\right)}{\rho_{\mathrm{A}}}\right) \left(\frac{\rho_{\mathrm{A}}}{\rho_{\mathrm{A}} - C_{\mathrm{A,eq}}}\right) \right] \\
&= \frac{V_{\mathrm{in}}}{m} (C_{\mathrm{A,in}} - C_{\mathrm{A,eq}}) \left[\frac{\rho_{\mathrm{A}} - \rho_{\mathrm{S}}}{\rho_{\mathrm{A}}} - \left(\frac{\rho_{\mathrm{A}} - \rho_{\mathrm{S}} - C_{\mathrm{A,eq}} + C_{\mathrm{A,eq}} \frac{\rho_{\mathrm{S}}}{\rho_{\mathrm{A}}}}{\rho_{\mathrm{A}} - C_{\mathrm{A,eq}}}\right) \right] \\
&= \frac{V_{\mathrm{in}}}{m} (C_{\mathrm{A,in}} - C_{\mathrm{A,eq}}) \left[\frac{(\rho_{\mathrm{A}} - \rho_{\mathrm{S}}) (\rho_{\mathrm{A}} - C_{\mathrm{A,eq}}) - \rho_{\mathrm{A}}\rho_{\mathrm{A}} + \rho_{\mathrm{A}}\rho_{\mathrm{S}} + \rho_{\mathrm{A}} C_{\mathrm{A,eq}} - C_{\mathrm{A,eq}}\rho_{\mathrm{S}}}{\rho_{\mathrm{A}} (\rho_{\mathrm{A}} - C_{\mathrm{A,eq}})} \right] \\
&= \frac{V_{\mathrm{in}}}{m} (C_{\mathrm{A,in}} - C_{\mathrm{A,eq}}) \left[\frac{(\rho_{\mathrm{A}} - \rho_{\mathrm{S}}) (\rho_{\mathrm{A}} - C_{\mathrm{A,eq}}) - (\rho_{\mathrm{A}} - \rho_{\mathrm{S}}) (\rho_{\mathrm{A}} - C_{\mathrm{A,eq}})}{\rho_{\mathrm{A}} (\rho_{\mathrm{A}} - C_{\mathrm{A,eq}})} \right] \\
&= 0
\end{aligned} \tag{13}$$

Therefore, the solvent loading calculated by the VC approach will always be zero when the solution density is calculated assuming ideal solution.

S2 Supplementary Results

S2.1 Adsorbent Characterization

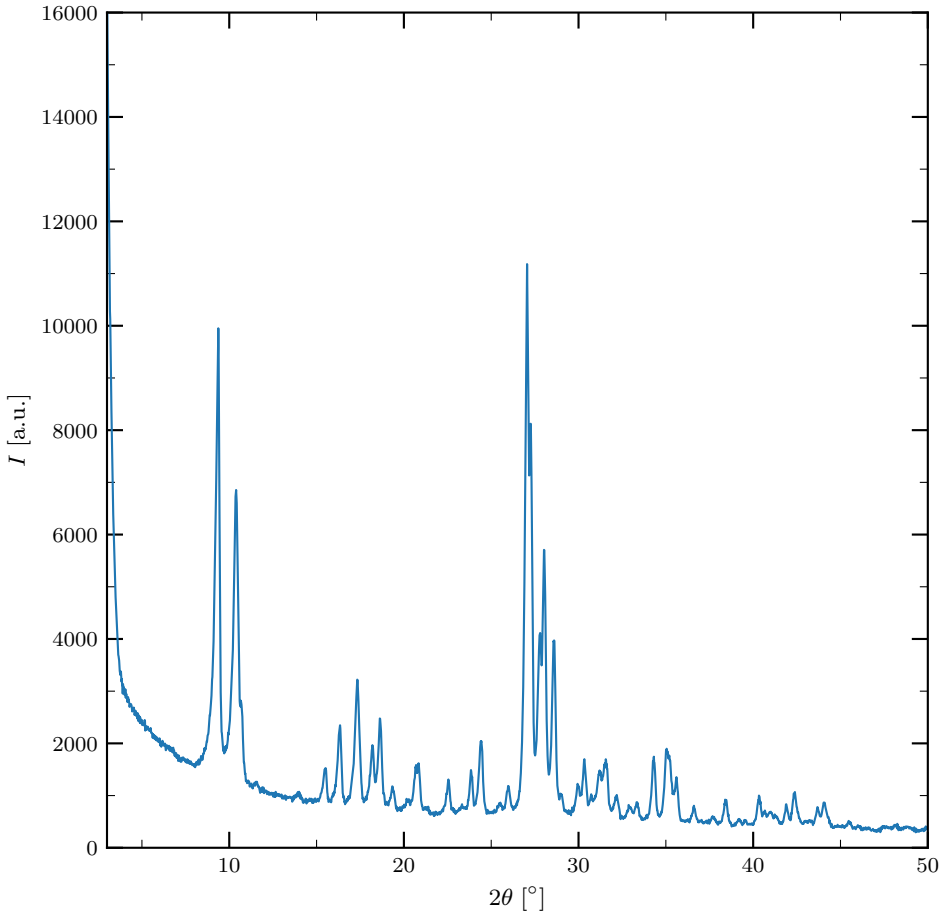

Figure S3: PXRD pattern of MFI-OH adsorbent.

(a)

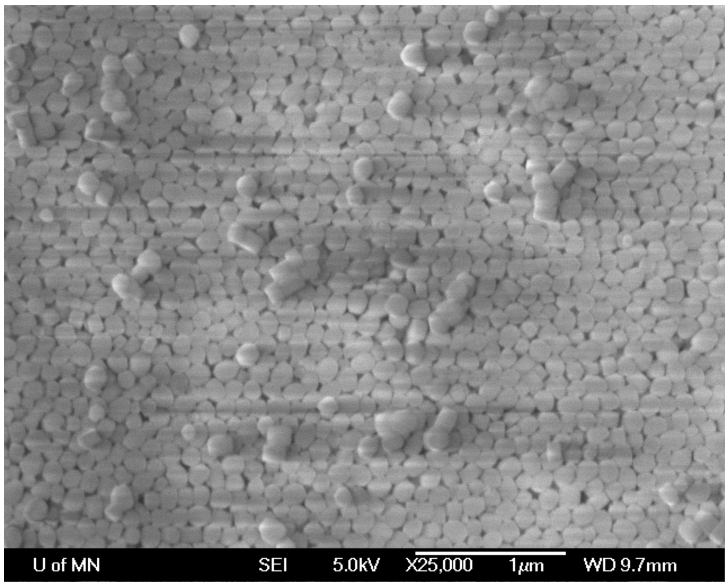

(b)

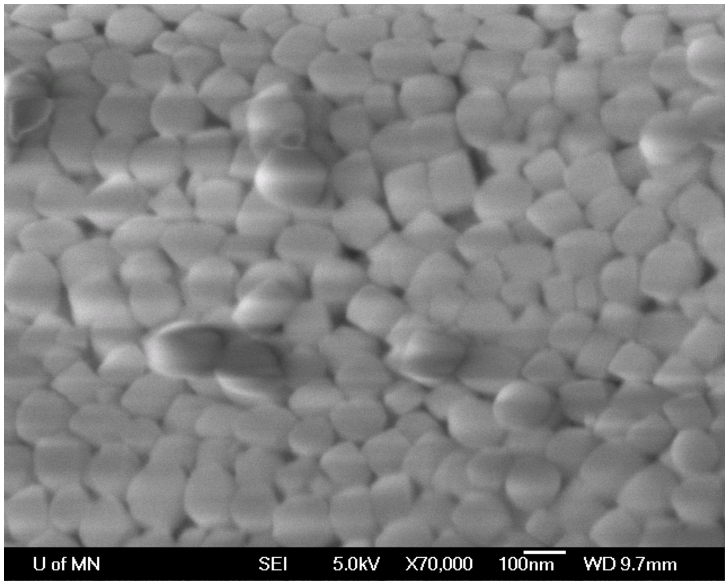

Figure S4: SEM images of MFI-OH crystals.

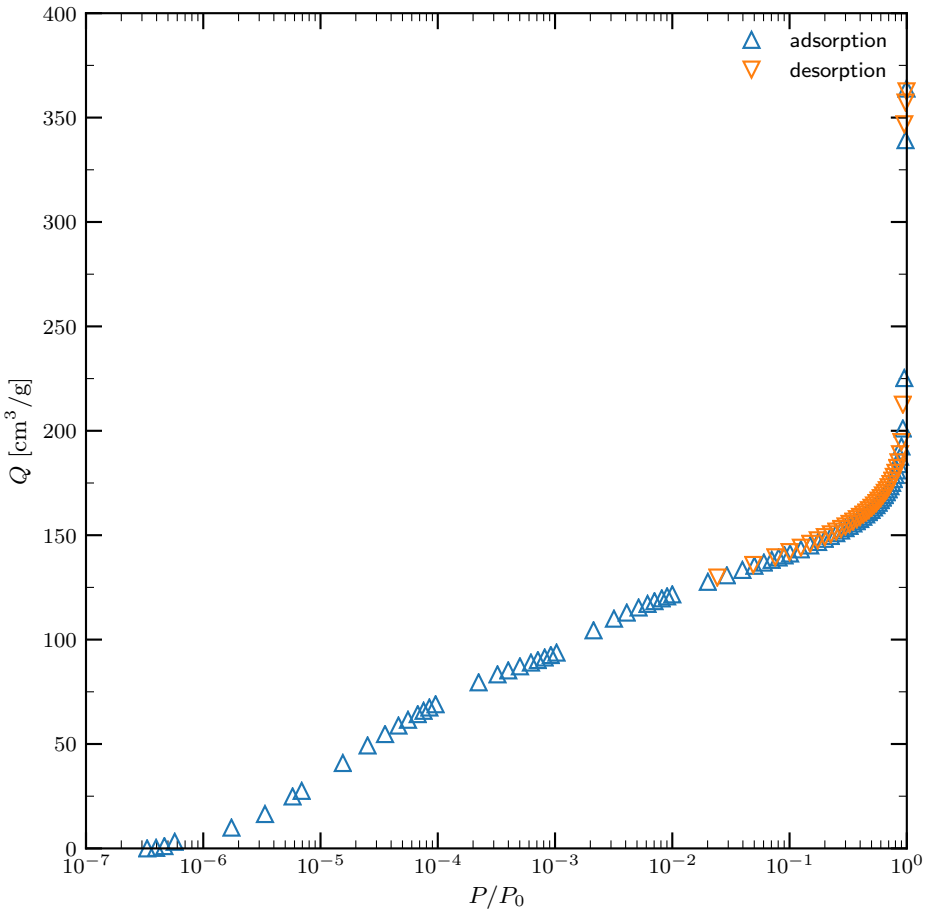

Figure S5: Ar adsorption/desorption isotherms of MFI-OH adsorbent at $T = 87$ K.

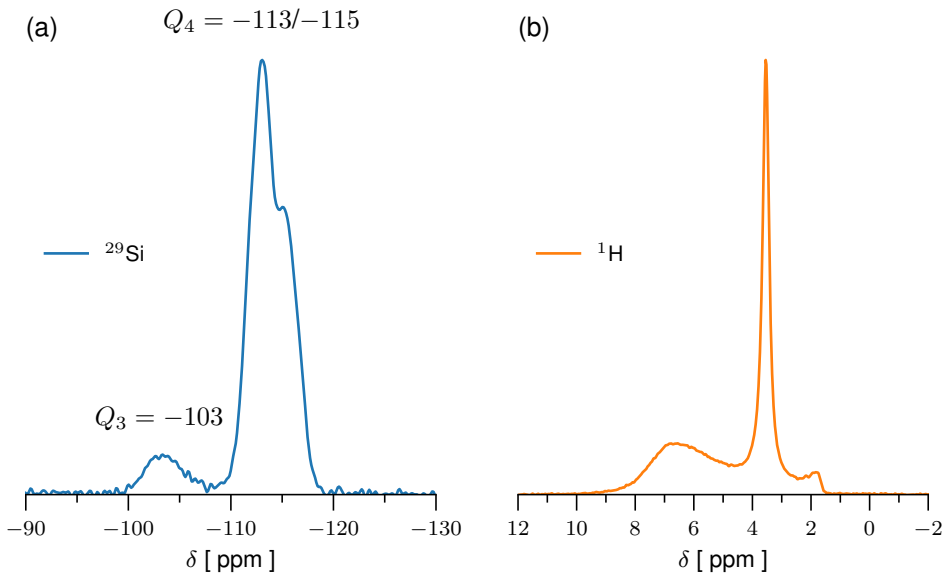

Figure S6: (a) ^{29} Si MAS solid-state NMR and (b) ^{1} H MAS solid-state NMR obtained on MFI-OH material.

S2.2 Adsorption Isotherms

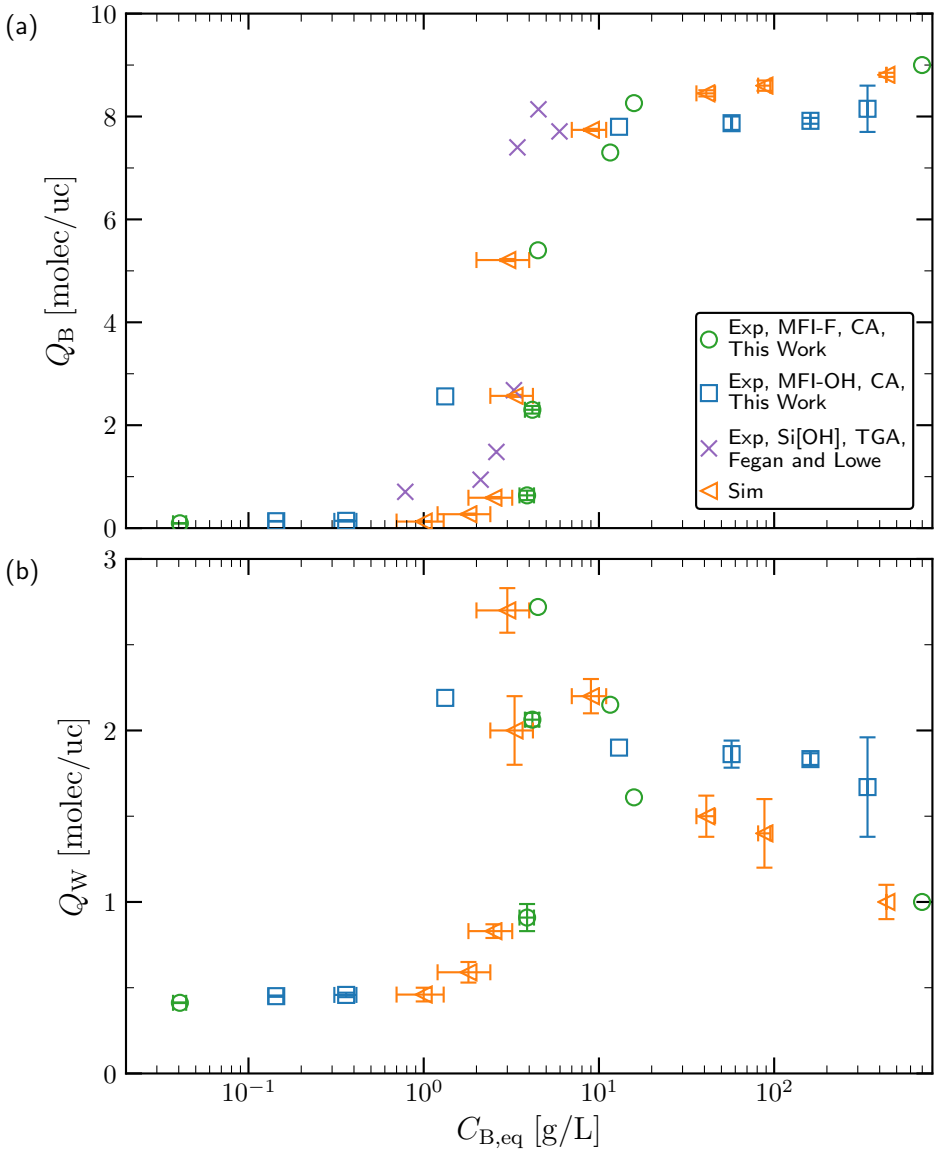

Figure S7: Equilibrium loadings of (a) butane-1,4-diol (B), and (b) water (W) as a function of solution concentration as obtained by simulations,[S8] experimentally by the coadsorption method for both the MFI-F and MFI-OH materials, and as reported by Fegan and Lowe who calculated the solute adsorption by thermal gravimetric analysis.[S9]

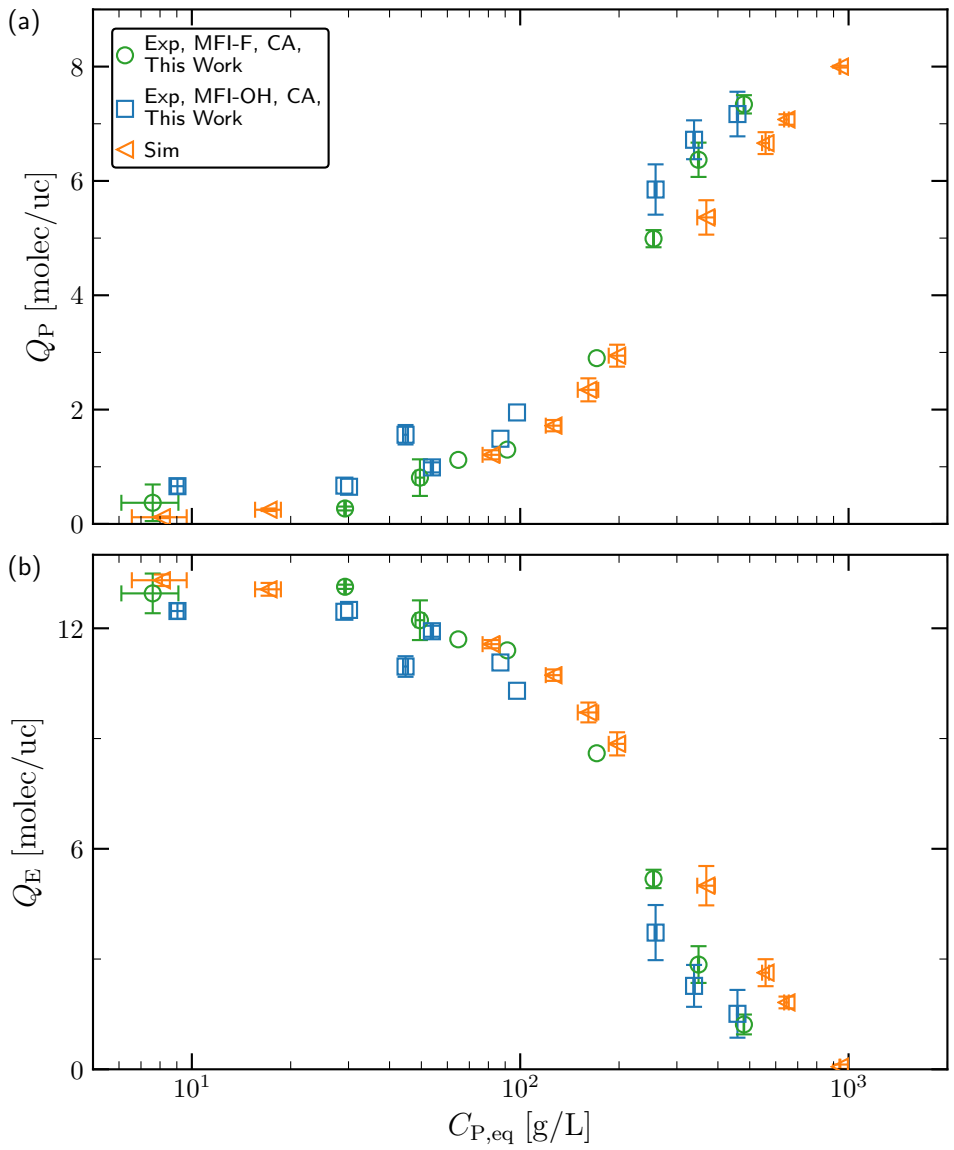

Figure S8: Equilibrium loadings of (a) pentane-1,5-diol (P), and (b) ethanol (E) as a function of solution concentration as obtained by simulation and experimentally by the coadsorption method for MFI-OH and MFI-F.

S2.3 Calculation of Uptake by Density Bottle Method

Table S3: Experimental Measurement and Calculations of Adsorption of P/W Mixtures onto MFI-OH at $T = 323$ K by the Density Bottle Method

	Data Point Label	
Property	80	81
$C_{\mathrm{A,in}}$ [g/mL]	0.6053 ± 0.0053	0.012162 ± 0.000014
$C_{\mathrm{A,eq}}$ [g/mL]	0.5982 ± 0.0068	0.0002891 ± 0.00000027
V_{f} [mL]	24.879 ± 0.001	24.865 ± 0.001
ρ_{in} [g/mL]	0.9905 ± 0.0001^a	0.9892 ± 0.0001^a
ρ_{eq} [g/mL]	0.9905 ± 0.0001^a	0.9892 ± 0.0001^a
$m_{\mathrm{l,o}}$ [g]	23.812 ± 0.001	23.755 ± 0.001
$m_{\mathrm{l,r}}$ [g]	0.5181 ± 0.0001	0.6432 ± 0.0001
m_{z} [g]	3.2203 ± 0.0001	3.3183 ± 0.0001
Q_{A} [molec/uc]	7.7 ± 3.5^a	4.758 ± 0.0058^a
Q_{S} [molec/uc]	1 ± 20^a	9.1 ± 1.1^a
ρ_{in} [g/mL]	1.0024 ± 0.00055^b	0.9972 ± 0.0002^b
ρ_{eq} [g/mL]	0.9982 ± 0.0005^b	0.9934 ± 0.0002^b
Q_{A} [molec/uc]	4.8 ± 3.5^b	4.7190 ± 0.0058^b
Q_{S} [molec/uc]	1 ± 20^b	0.1 ± 1.1^b

[a]Calculated using densities at $T = 323$ K, as depicted in Figure S2.
[b]Calculated using densities at $T = 298$ K, measured at each associated concentration.

Table S4: Experimental Measurement and Calculations of Adsorption of P/E Mixtures onto MFI-OH at $T = 323$ K by the Density Bottle Method

	Data Point Label	
Property	82	83
$C_{\mathrm{A,in}}$ [g/mL]	0.04069 ± 0.00065	0.2465 ± 0.0059
$C_{\mathrm{A,eq}}$ [g/mL]	0.04006 ± 0.00040	0.2522 ± 0.0038
V_{f} [mL]	24.835 ± 0.001	24.857 ± 0.001
ρ_{in} [g/mL]	0.7721 ± 0.0001	0.8182 ± 0.0013
ρ_{eq} [g/mL]	0.7723 ± 0.0001	0.8195 ± 0.0008
$m_{\mathrm{l,o}}$ [g]	19.007 ± 0.001	20.048 ± 0.001
$m_{\mathrm{l,r}}$ [g]	0.3047 ± 0.0001	0.1995 ± 0.0001
m_{z} [g]	3.1612 ± 0.0001	3.1408 ± 0.0001
Q_{A} [molec/uc]	0.57 ± 0.32	7.6 ± 2.9
Q_{S} [molec/uc]	34.70 ± 0.78	20.3 ± 6.7

S2.4 Options for Coadsorption Models for Si-OH without Simulation

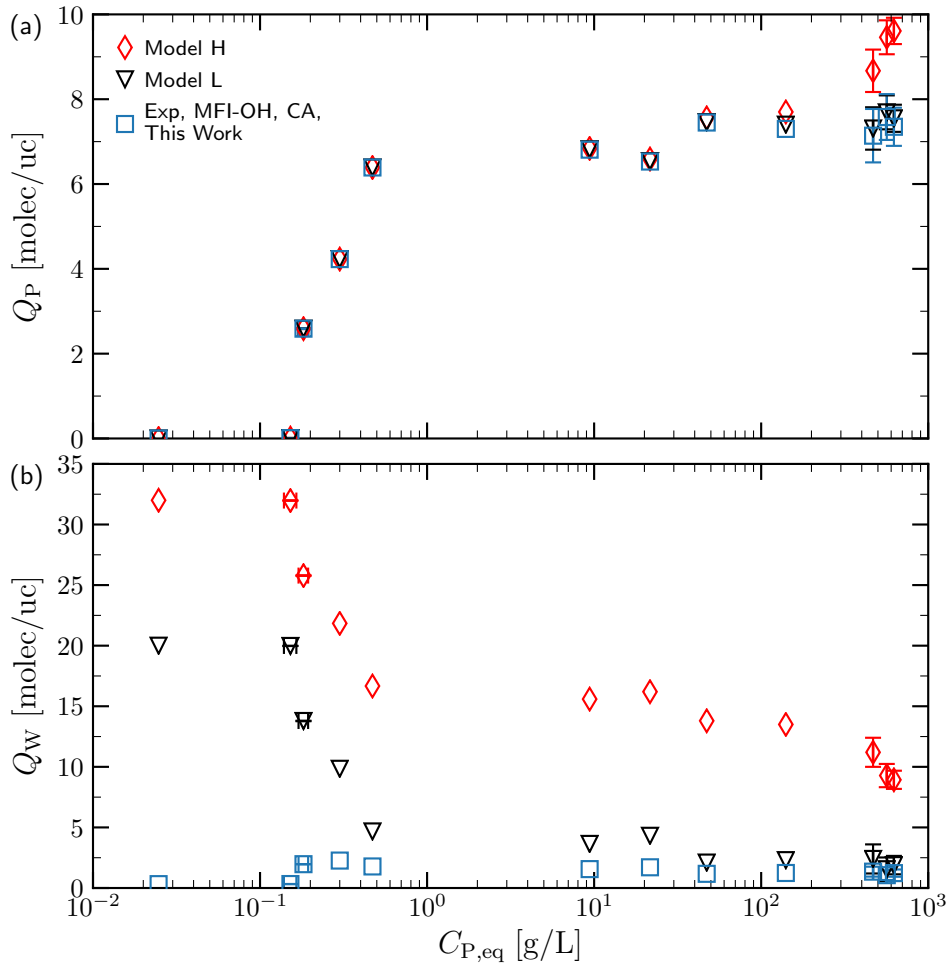

Figure S9: Adsorption of (a) pentane-1,5-diol and (b) water from aqueous solution, as calculated by two different coadsorption models (H and L) and compared to the coadsorption model determined by simulation of the defect-free structure. In Model H, the coadsorption fit is chosen so that a_0, the neat solvent loading, is 32, while, for Model L, $a_0 = 20$ molec solvent / uc. For both models, $a_1 = -2.4$ molec solvent / molec diol.

S2.5 Calculation Method Sensitivities

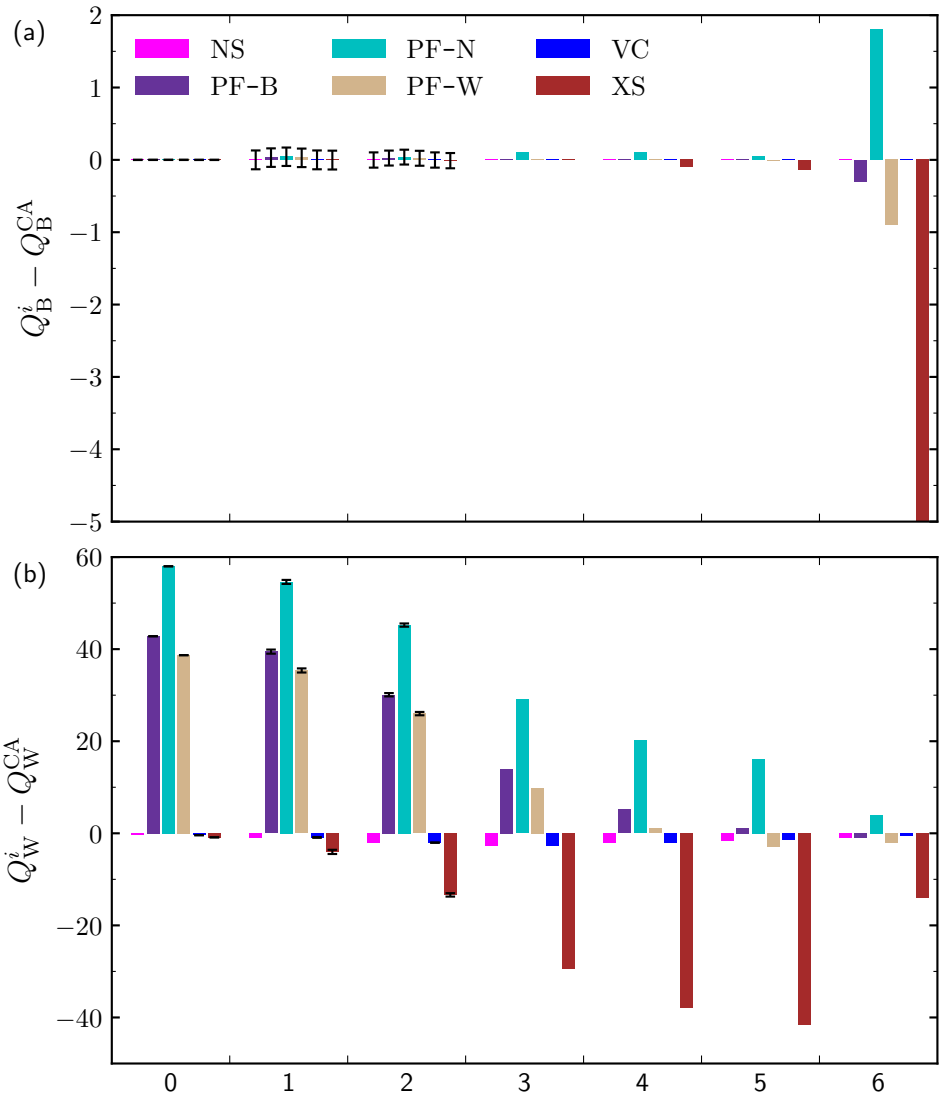

Figure S10: Difference between NS, PF-B, PF-N, PF-W, VC, or XS (superscript i) and the coadsorption approach (CA) for (a) butane-1,4-diol (B) loading and (b) water (W) loading at different solution concentrations (and loadings) increasing in value from left-to-right. All loadings are presented in units of molec/uc, and the x-axis ticks separate different state points, Error bars (black) are present in the cases where replicate experimental measurements were performed.

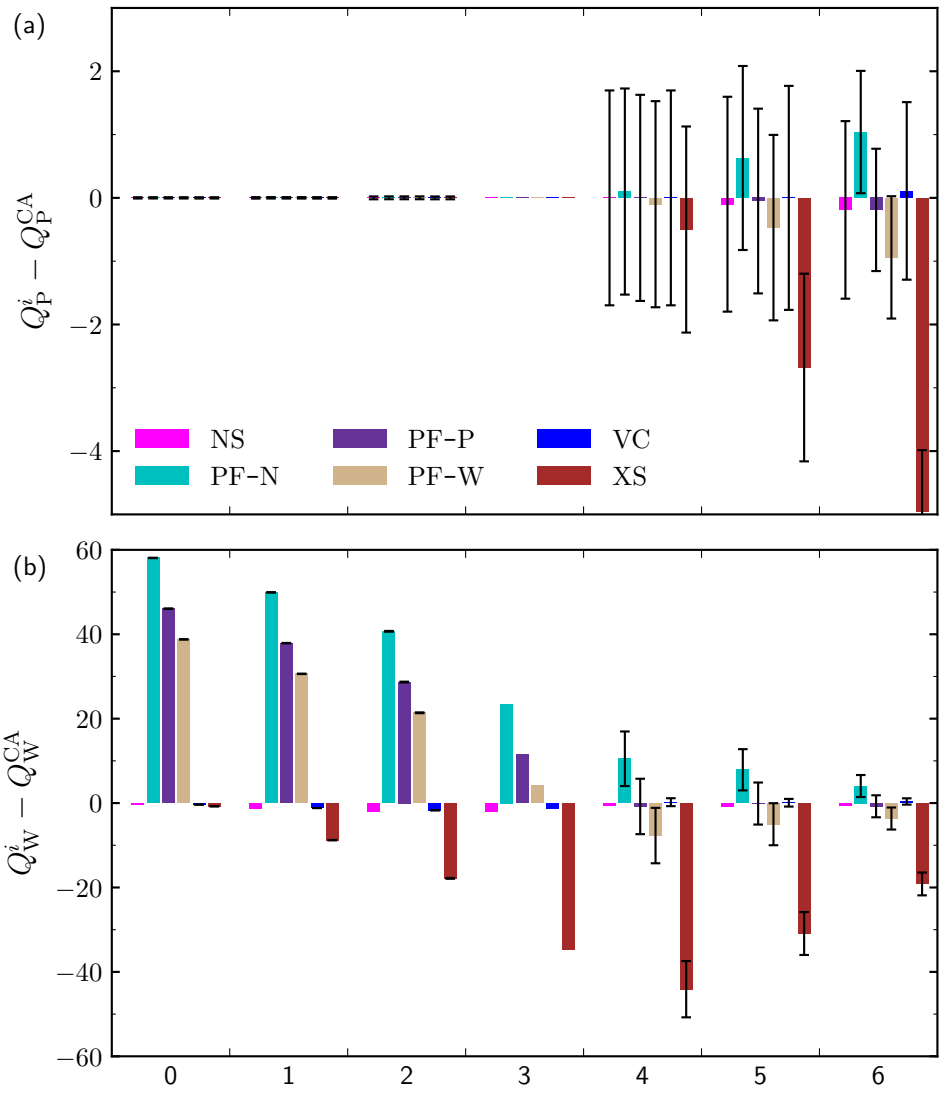

Figure S11: As Figure S10 for the P/W mixture.

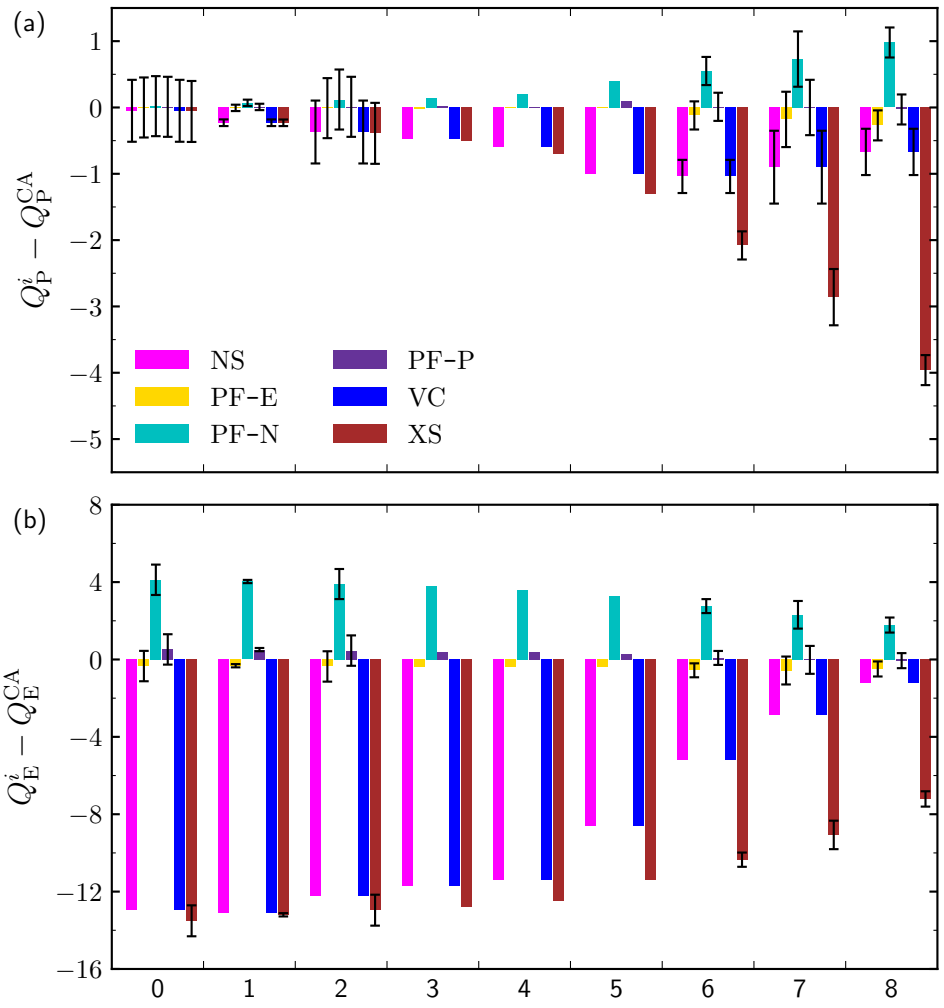

Figure S12: As Figure S10 for the P/E mixture.

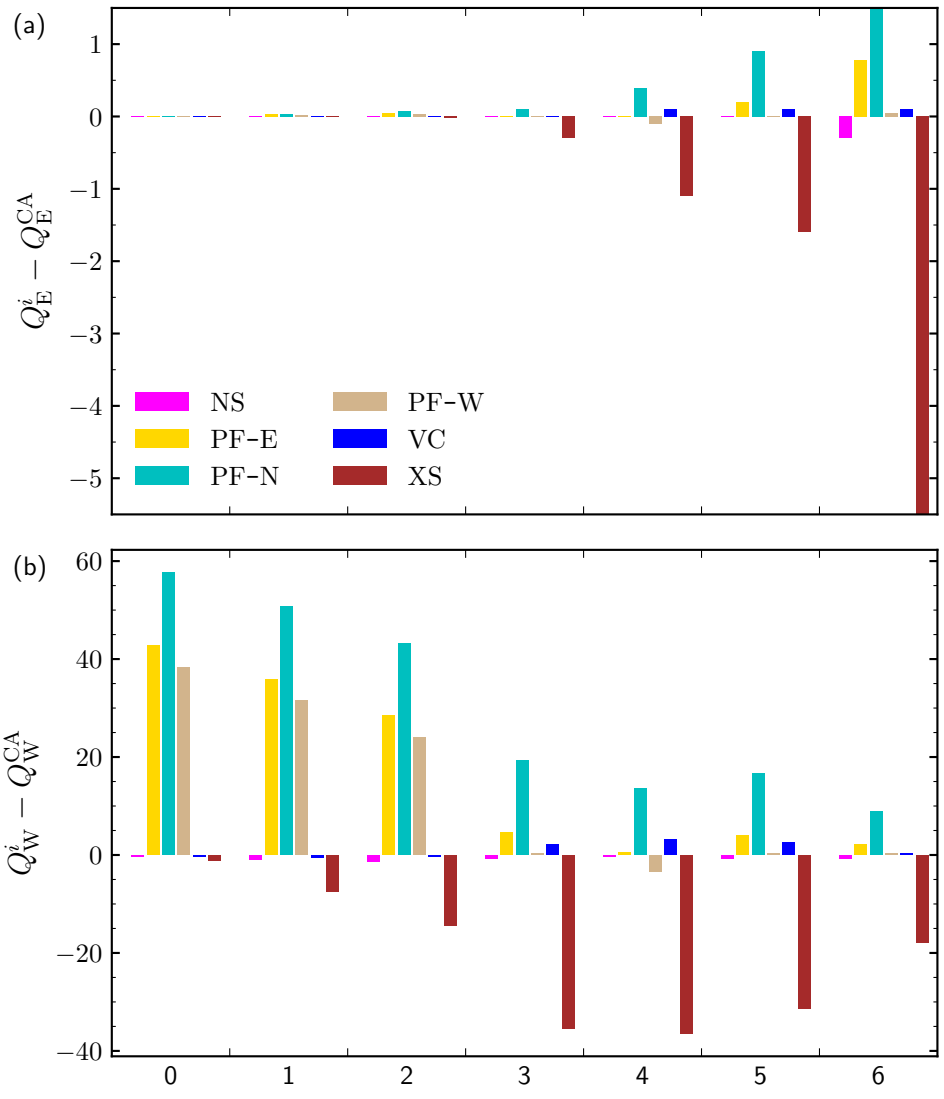

Figure S13: As Figure S10 for the E/W mixture.

S2.6 Tables of Simulated Liquid-Phase Adsorption Equilibria

Table S5: Adsorption of Pentane-1,5-Diol/Ethanol onto silicalite-1 at $T = 323$ K and $p = 1.0$ bar obtained from simulations using an explicit liquid solution-phase and a gas-phase transfer medium.

Mean			95% Confidence		
$C_{\mathrm{P,eq}}$ [g / L]	Q_{P} [molec / uc]	Q_{E} [molec / uc]	$C_{\mathrm{P,eq}}$ [g / L]	Q_{P} [molec / uc]	Q_{E} [molec / uc]
8.1	0.117	13.31	1.5	0.015	0.16
17.1	0.25	13.06	1.5	0.02	0.17
82	1.21	11.57	5	0.08	0.11
126	1.7	10.73	7	0.1	0.16
161	2.3	9.7	12	0.2	0.3
197	2.94	8.9	11	0.19	0.3
370	5.4	5.0	20	0.3	0.5
559	6.66	2.6	14	0.19	0.4
647	7.08	1.82	11	0.09	0.16
941	7.999	0.07	3	0.015	0.06

Other raw data points for P/W and B/W were reported in the Supplementary Material of previous work.[S8]

S2.7 Tables of Unary Vapor-Phase Adsorption Equilibria

Table S6: Adsorption of Ethanol at 298 K onto MFI-F.[a]

P [Pa]	Q_{E} [molec/uc]
118	8.4
275	10.7
393	11.3
511	11.8
669	12.2
787	12.5
1180	13.0
1570	13.3
2360	13.7
3150	13.9
3930	14.1
4720	14.2
5510	14.3
6300	14.3
7080	14.4

[a]Pressures are calculated using a saturation vapor pressure of 7869 Pa (Ref. S10).

Table S7: Adsorption of Ethanol at 298 K onto MFI-OH.[a]

P [Pa]	Q_{E} [molec/uc]
118	11.8
275	13.9
393	14.6
511	15.0
669	15.4
787	15.7
1180	16.3
1570	16.7
2360	17.3
3150	17.6
3930	17.9
4720	18.1
5510	18.4
6300	18.9
7080	21.6

[a]Pressures are calculated using a saturation vapor pressure of 7869 Pa (Ref. S10).

Table S8: Adsorption of Water at 298 K onto MFI-F.[a]

P [Pa]	Q_{W} [molec/uc]
4.71	0.00
78.2	0.12
160	0.14
314	0.19
469	0.24
627	0.26
775	0.29
947	0.36
1100	0.41
1260	0.45
1580	0.55
1890	0.75
2180	0.92
2490	1.09
2880	1.28
2960	1.45

[a]Pressures are calculated using a saturation vapor pressure of 3141 Pa (Ref. S11).

Table S9: Adsorption of Water at 298 K onto MFI-OH.[a]

P [Pa]	Q_{W} [molec/uc]
2.51	0.00
79.2	1.65
158	2.37
314	3.89
472	5.20
627	6.62
784	8.13
941	9.36
1100	10.4
1260	11.4
1580	13.0
1880	14.5
2200	16.0
2510	18.0
2830	22.1
2980	31.7

[a]Pressures are calculated using a saturation vapor pressure of 3141 Pa (Ref. S11).

S2.8 Raw Data Tables of Liquid-Phase Adsorption Measurements

Table S10: Measurements for Adsorption of E/W at 323 K onto MFI-F.[a]

Label	$C_{\mathrm{E,in}}$ [g/L]	$C_{\mathrm{E,eq}}$ [g/L]	m [g]	V_i [mL]
121-1	0.626 ± 0.047	0.13 ± 0.11	0.1007 ± 0.0001	0.400 ± 0.001
121-4	6.02 ± 0.40	1.73 ± 0.65	0.1004 ± 0.0001	0.400 ± 0.001
121-6	12.7 ± 1.2	4.180 ± 0.048	0.1003 ± 0.0001	0.400 ± 0.001
121-7	40.2 ± 1.5	17.7 ± 1.7	0.0996 ± 0.0001	0.400 ± 0.001
121-9	91.36 ± 0.90	67 ± 12	0.1003 ± 0.0001	0.400 ± 0.001
121-10	130.5 ± 3.1	110.4 ± 1.3	0.0999 ± 0.0001	0.400 ± 0.001
121-15	440.97 ± 0.90	430.8 ± 1.3	0.1003 ± 0.0001	0.400 ± 0.001

[a] Uncertainties in concentrations are determined from multiple GC injections unless otherwise noted.

Table S11: Measurements for Adsorption of B/W at 323 K onto MFI-OH.[a]

Label	$C_{\mathrm{B,in}}$ [g/L]	$C_{\mathrm{B,eq}}$ [g/L]	m [g]	V_i [mL]
78-1	0.0350 ± 0.0022	0.00133 ± 0.00033	0.0997 ± 0.0001	0.400 ± 0.001
78-2	0.0350 ± 0.0022	0.00133 ± 0.00081	0.0997 ± 0.0001	0.400 ± 0.001
78-3	0.0350 ± 0.0022	0.00179 ± 0.00089	0.1002 ± 0.0001	0.400 ± 0.001
78-6	0.666 ± 0.044	0.128 ± 0.028	0.0996 ± 0.0001	0.400 ± 0.001
78-5	0.666 ± 0.044	0.148 ± 0.017	0.0999 ± 0.0001	0.400 ± 0.001
78-4	0.666 ± 0.031	0.155 ± 0.086	0.1000 ± 0.0001	0.400 ± 0.001
78-7	0.912 ± 0.018	0.325 ± 0.029	0.0996 ± 0.0001	0.400 ± 0.001
78-8	0.912 ± 0.018	0.40 ± 0.10	0.1000 ± 0.0001	0.400 ± 0.001
78-9	11.31 ± 0.85	1.327 ± 0.045	0.1000 ± 0.0001	0.400 ± 0.001
78-11	43.23 ± 0.78	13.02 ± 0.37	0.1005 ± 0.0001	0.400 ± 0.001
78-13	86 ± 10	56.88 ± 0.46	0.0996 ± 0.0001	0.400 ± 0.001
78-14	86 ± 10	57.4 ± 3.0	0.1002 ± 0.0001	0.400 ± 0.001
78-15	187 ± 19	161 ± 15	0.1006 ± 0.0001	0.400 ± 0.001
78-16	187 ± 19	161.0 ± 6.8	0.1003 ± 0.0001	0.400 ± 0.001
78-17	187 ± 19	161 ± 11	0.1005 ± 0.0001	0.400 ± 0.001
78-19	362 ± 16	340.1 ± 2.1	0.1000 ± 0.0001	0.400 ± 0.001
78-18	362 ± 16	340.6 ± 1.3	0.1004 ± 0.0001	0.400 ± 0.001
78-20	362 ± 16	342 ± 12	0.1004 ± 0.0001	0.400 ± 0.001

[a] Replicate experiments are separated in rows with horizontal lines. Uncertainties in concentrations are determined from multiple GC injections.

Table S12: Measurements for Adsorption of B/W at 323 K onto MFI-F.[a]

Label	$C_{\mathrm{B,in}}$ [g/L]	$C_{\mathrm{B,eq}}$ [g/L]	m [g]	V_i [mL]
118-2	0.408 ± 0.024	0.038 ± 0.029	0.0997 ± 0.0001	0.400 ± 0.001
118-1	0.408 ± 0.024	0.043 ± 0.014	0.1006 ± 0.0001	0.400 ± 0.001
118-6	13.11 ± 0.54	3.9 ± 2.0	0.1007 ± 0.0001	0.400 ± 0.001
118-5	13.11 ± 0.54	4.5 ± 1.3	0.0991 ± 0.0001	0.400 ± 0.001
118-4	6.37 ± 0.70	3.63 ± 0.41	0.1005 ± 0.0001	0.400 ± 0.001
118-3	6.37 ± 0.70	4.15 ± 0.31	0.1000 ± 0.0001	0.400 ± 0.001
122-3	25.4 ± 4.2	4.49 ± 0.19	0.0992 ± 0.0001	0.400 ± 0.001
122-4	40.2 ± 7.2	11.6 ± 1.9	0.1008 ± 0.0001	0.400 ± 0.001
122-5	47.67 ± 0.78	15.85 ± 0.75	0.1002 ± 0.0001	0.400 ± 0.001
118-9	708 ± 16	698 ± 20	0.0996 ± 0.0001	0.400 ± 0.001

[a] Replicate experiments are separated in rows with horizontal lines. Uncertainties in concentrations are determined from multiple GC injections.

Table S13: Measurements for Adsorption of P/W at 323 K onto MFI-OH.[a]

Label	$C_{\mathrm{P,in}}$ [g/L]	$C_{\mathrm{P,eq}}$ [g/L]	m [g]	V_i [mL]
15-1	0.0250 ± 0.0022	0.0247 ± 0.0022	0.0987 ± 0.0001	0.400 ± 0.001
76-3	0.191 ± 0.016	0.137 ± 0.017	0.0998 ± 0.0001	0.400 ± 0.001
76-2	0.191 ± 0.016	0.160 ± 0.029	0.1004 ± 0.0001	0.400 ± 0.001
15-2	0.191 ± 0.016	0.160 ± 0.043	0.0993 ± 0.0001	0.400 ± 0.001
76-6	11.95 ± 0.50	0.17 ± 0.14	0.1004 ± 0.0001	0.400 ± 0.001
15-7	11.95 ± 0.50	0.177 ± 0.012	0.1010 ± 0.0001	0.400 ± 0.001
76-5	11.95 ± 0.50	0.20 ± 0.11	0.1006 ± 0.0001	0.400 ± 0.001
15-8[b]	20.00 ± 0.50	0.300 ± 0.022	0.1031 ± 0.0001	0.400 ± 0.001
15-9[b]	30.00 ± 0.75	0.471 ± 0.054	0.1024 ± 0.0001	0.400 ± 0.001
15-10[b]	40.0 ± 1.0	9.40 ± 0.10	0.1004 ± 0.0001	0.400 ± 0.001
15-11[b]	50.0 ± 1.2	21.6 ± 1.3	0.0986 ± 0.0001	0.400 ± 0.001
15-12[b]	80.0 ± 2.0	47.2 ± 3.5	0.1024 ± 0.0001	0.400 ± 0.001
15-13[b]	170.0 ± 4.2	140.5 ± 2.4	0.1042 ± 0.0001	0.400 ± 0.001
76-7	484.2 ± 6.7	466 ± 12	0.1001 ± 0.0001	0.400 ± 0.001
76-9	484.2 ± 6.7	468.5 ± 2.5	0.1000 ± 0.0001	0.400 ± 0.001
76-8	484.2 ± 6.7	468.7 ± 6.3	0.0998 ± 0.0001	0.400 ± 0.001
76-12	579 ± 12	563.5 ± 7.2	0.1000 ± 0.0001	0.400 ± 0.001
76-10	579 ± 12	565 ± 17	0.1000 ± 0.0001	0.400 ± 0.001
76-11	579 ± 12	566 ± 19	0.0997 ± 0.0001	0.400 ± 0.001
76-14	635 ± 13	622.55 ± 0.40	0.1004 ± 0.0001	0.400 ± 0.001
76-13	635 ± 13	623.9 ± 2.6	0.1007 ± 0.0001	0.400 ± 0.001

[a] Replicate experiments are separated in rows with horizontal lines. Uncertainties in concentrations are determined from multiple GC injections unless otherwise noted.
[b] Initial concentration is nominal concentration. Uncertainty in initial concentration is estimated assuming that the relative error in concentration is similar to those at similar concentrations.

Table S14: Measurements for Adsorption of P/W at 323 K onto MFI-F.[a]

Label	$C_{\mathrm{P,in}}$ [g/L]	$C_{\mathrm{P,eq}}$ [g/L]	m [g]	V_i [mL]
117-2	0.3721 ± 0.0042	0.0487 ± 0.0078	0.1005 ± 0.0001	0.400 ± 0.001
117-1	0.3721 ± 0.0042	0.097 ± 0.014	0.1000 ± 0.0001	0.400 ± 0.001
117-4	5.95 ± 0.41	0.100 ± 0.024	0.0996 ± 0.0001	0.400 ± 0.001
117-3	5.95 ± 0.41	0.116 ± 0.022	0.1002 ± 0.0001	0.400 ± 0.001
117-5	12.54 ± 0.12	0.130 ± 0.018	0.0997 ± 0.0001	0.400 ± 0.001
117-6	12.54 ± 0.12	0.160 ± 0.023	0.1003 ± 0.0001	0.400 ± 0.001
119-1	25.68 ± 0.29	0.24 ± 0.16	0.0994 ± 0.0001	0.400 ± 0.001
119-4	90.9 ± 9.8	53 ± 31	0.1004 ± 0.0001	0.400 ± 0.001
119-3	90.9 ± 9.8	60 ± 26	0.1005 ± 0.0001	0.400 ± 0.001
117-7	349.9 ± 4.1	324 ± 13	0.0995 ± 0.0001	0.400 ± 0.001
117-8	349.9 ± 4.1	329.24 ± 0.85	0.0992 ± 0.0001	0.400 ± 0.001
117-9	609 ± 11	593 ± 42	0.1003 ± 0.0001	0.400 ± 0.001
117-10	609 ± 11	595 ± 24	0.1002 ± 0.0001	0.400 ± 0.001

[a] Replicate experiments are separated in rows with horizontal lines. Uncertainties in concentrations are determined from multiple GC injections unless otherwise noted.

Table S15: Measurements for Adsorption of P/E at 323 K onto MFI-OH.[a]

Label	$C_{\mathrm{P,in}}$ [g/L]	$C_{\mathrm{P,eq}}$ [g/L]	m [g]	V_i [mL]
77-1	11.83 ± 0.74	8.78 ± 0.28	0.1009 ± 0.0001	0.400 ± 0.001
77-2	11.83 ± 0.74	8.84 ± 0.39	0.1008 ± 0.0001	0.400 ± 0.001
34-1	11.50 ± 0.74	9.50 ± 0.50	0.1006 ± 0.0001	0.400 ± 0.001
77-3	31.13 ± 0.64	29.14 ± 0.23	0.0998 ± 0.0001	0.400 ± 0.001
34-2	31.97 ± 0.64	30.11 ± 0.20	0.1008 ± 0.0001	0.400 ± 0.001
77-4	50.2 ± 2.4	44.2 ± 2.0	0.1003 ± 0.0001	0.400 ± 0.001
77-5	50.2 ± 2.4	45.3 ± 2.7	0.1004 ± 0.0001	0.400 ± 0.001
34-3	56.4 ± 1.5	53.5 ± 1.5	0.1006 ± 0.0001	0.400 ± 0.001
34-4	56.4 ± 1.5	54.1 ± 2.4	0.1001 ± 0.0001	0.400 ± 0.001
34-5	90.67 ± 0.83	87.04 ± 0.20	0.1001 ± 0.0001	0.400 ± 0.001
34-6	103.06 ± 0.93	97.78 ± 0.20	0.0998 ± 0.0001	0.400 ± 0.001
77-6	276 ± 14	256.69 ± 0.90	0.0998 ± 0.0001	0.400 ± 0.001
34-8	274 ± 14	258.2 ± 4.3	0.0995 ± 0.0001	0.400 ± 0.001
77-7	276 ± 14	260.3 ± 7.4	0.0996 ± 0.0001	0.400 ± 0.001
77-8	356.2 ± 9.9	337.2 ± 9.3	0.1005 ± 0.0001	0.400 ± 0.001
34-19	356.4 ± 9.9	339.7 ± 7.0	0.1004 ± 0.0001	0.400 ± 0.001
77-10	474.1 ± 3.3	457.6 ± 9.1	0.0999 ± 0.0001	0.400 ± 0.001
77-9	474.1 ± 3.3	460.1 ± 2.0	0.1000 ± 0.0001	0.400 ± 0.001

[a] Replicate experiments are separated in rows with horizontal lines. Uncertainties in concentrations are determined from multiple GC injections.

Table S16: Measurements for Adsorption of P/E at 323 K onto MFI-F.[a]

Label	$C_{P,in}$ [g/L]	$C_{P,eq}$ [g/L]	m [g]	V_i [mL]
115-1	9.042 ± 0.032	6.6 ± 2.8	0.1001 ± 0.0001	0.400 ± 0.001
115-2	9.042 ± 0.032	8.69 ± 0.10	0.1006 ± 0.0001	0.400 ± 0.001
115-4	29.4 ± 1.6	29.16 ± 0.30	0.0992 ± 0.0001	0.400 ± 0.001
115-3	29.4 ± 1.6	29.39 ± 0.67	0.1001 ± 0.0001	0.400 ± 0.001
115-6	51.4 ± 3.5	48.4 ± 9.2	0.0996 ± 0.0001	0.400 ± 0.001
115-5	51.4 ± 3.5	50.5 ± 2.0	0.1007 ± 0.0001	0.400 ± 0.001
115-7	67.5 ± 2.9	64.8 ± 0	0.0995 ± 0.0001	0.400 ± 0.001
115-8	94.0 ± 8.8	91.3 ± 3.3	0.1001 ± 0.0001	0.400 ± 0.001
115-9	178 ± 15	171 ± 13	0.1014 ± 0.0001	0.400 ± 0.001
115-10	268 ± 17	254.2 ± 5.3	0.0995 ± 0.0001	0.400 ± 0.001
115-11	268 ± 17	255.2 ± 8.4	0.0996 ± 0.0001	0.400 ± 0.001
115-13	365 ± 20	348.3 ± 7.2	0.1000 ± 0.0001	0.400 ± 0.001
115-12	365 ± 20	350.2 ± 9.6	0.1003 ± 0.0001	0.400 ± 0.001
115-15	495 ± 27	479.6 ± 5.7	0.1002 ± 0.0001	0.400 ± 0.001
115-14	495 ± 27	480.6 ± 2.7	0.1001 ± 0.0001	0.400 ± 0.001

[a] Replicate experiments are separated in rows with horizontal lines. Uncertainties in concentrations are determined from multiple GC injections unless otherwise noted.

S2.9 Tables from Calculation of Experimental Uptakes

Table S17: Loadings (units of molec/uc) at Low Concentrations (units of g/L) of B/W onto MFI-OH at 323 K.

$C_{\mathrm{B,eq}}$	0.00148 ± 0.00027^{r}	0.144 ± 0.014^{r}	0.361 ± 0.052^{r}	1.327 ± 0.045^{s}	13.02 ± 0.37^{s}
$Q_{\mathrm{B}}^{\mathrm{CA}}$	$0.008578 \pm 0.000093^{r}$	0.1340 ± 0.0038^{r}	0.141 ± 0.014^{r}	2.56 ± 0.22^{s}	7.80 ± 0.22^{s}
$Q_{\mathrm{B}}^{\mathrm{NS}}$	$0.008578 \pm 0.000093^{r}$	0.1340 ± 0.0038^{r}	0.141 ± 0.014^{r}	2.56 ± 0.22^{s}	7.79 ± 0.22^{s}
$Q_{\mathrm{B}}^{\mathrm{PF-B}}$	$0.008591 \pm 0.000091^{r}$	0.1352 ± 0.0037^{r}	0.144 ± 0.013^{r}	2.57 ± 0.22^{s}	7.81 ± 0.22^{s}
$Q_{\mathrm{B}}^{\mathrm{PF-N}}$	$0.008595 \pm 0.000090^{r}$	0.1357 ± 0.0037^{r}	0.146 ± 0.013^{r}	2.57 ± 0.22^{s}	7.85 ± 0.22^{s}
$Q_{\mathrm{B}}^{\mathrm{PF-W}}$	$0.008589 \pm 0.000091^{r}$	0.1351 ± 0.0037^{r}	0.144 ± 0.013^{r}	2.57 ± 0.22^{s}	7.79 ± 0.22^{s}
$Q_{\mathrm{B}}^{\mathrm{VC}}$	$0.008578 \pm 0.000093^{r}$	0.1340 ± 0.0038^{r}	0.141 ± 0.014^{r}	2.56 ± 0.22^{s}	7.79 ± 0.22^{s}
$Q_{\mathrm{B}}^{\mathrm{XS}}$	$0.008578 \pm 0.000093^{r}$	0.1340 ± 0.0038^{r}	0.141 ± 0.014^{r}	2.55 ± 0.22^{s}	7.69 ± 0.22^{s}
$Q_{\mathrm{W}}^{\mathrm{CA}}$	$0.328417 \pm 0.000092^{r}$	0.4508 ± 0.0037^{r}	0.458 ± 0.013^{r}	2.19 ± 0.10^{s}	1.90 ± 0.13^{s}
$Q_{\mathrm{W}}^{\mathrm{PF-B}}$	43.63998 ± 0.00045^{r}	43.012 ± 0.018^{r}	42.967 ± 0.065^{r}	31.0 ± 1.1^{s}	5.0 ± 1.1^{s}
$Q_{\mathrm{W}}^{\mathrm{PF-N}}$	58.83389 ± 0.00045^{r}	58.204 ± 0.018^{r}	58.155 ± 0.065^{r}	46.1 ± 1.1^{s}	20.0 ± 1.1^{s}
$Q_{\mathrm{W}}^{\mathrm{PF-W}}$	39.52496 ± 0.00045^{r}	38.898 ± 0.018^{r}	38.853 ± 0.066^{r}	26.9 ± 1.1^{s}	0.9 ± 1.1^{s}
$Q_{\mathrm{W}}^{\mathrm{VC}}$	$[(9.60 \pm 0.10) \times 10^{-5}]^{r}$	$0.001529 \pm 0.000043^{r}$	0.00163 ± 0.00016^{r}	0.0376 ± 0.0038^{s}	0.2031 ± 0.0070^{s}
$Q_{\mathrm{W}}^{\mathrm{XS}}$	-0.04241 ± 0.00046^{r}	-0.662 ± 0.019^{r}	-0.698 ± 0.068^{r}	-12.6 ± 1.1^{s}	-37.9 ± 1.1^{s}

^{r} Uncertainty determined from replicate experiments.

^{s} Uncertainty estimated from linear error propagation.

Table S18: Loadings (units of molec/uc) at High Concentrations (units of g/L) of B/W onto MFI-OH at 323 K.

$C_{\mathrm{B,eq}}$	57.14 ± 0.38^{r}	161.08 ± 0.20^{r}	341.0 ± 1.3^{r}
$Q_{\mathrm{B}}^{\mathrm{CA}}$	7.87 ± 0.13^{r}	7.916 ± 0.057^{r}	8.15 ± 0.45^{r}
$Q_{\mathrm{B}}^{\mathrm{NS}}$	7.84 ± 0.13^{r}	7.845 ± 0.058^{r}	7.97 ± 0.48^{r}
$Q_{\mathrm{B}}^{\mathrm{PF-B}}$	7.90 ± 0.12^{r}	8.001 ± 0.049^{r}	8.26 ± 0.32^{r}
$Q_{\mathrm{B}}^{\mathrm{PF-N}}$	8.08 ± 0.12^{r}	8.495 ± 0.048^{r}	9.30 ± 0.31^{r}
$Q_{\mathrm{B}}^{\mathrm{PF-W}}$	7.85 ± 0.13^{r}	7.867 ± 0.049^{r}	7.98 ± 0.32^{r}
$Q_{\mathrm{B}}^{\mathrm{VC}}$	7.85 ± 0.13^{r}	7.869 ± 0.059^{r}	8.05 ± 0.49^{r}
$Q_{\mathrm{B}}^{\mathrm{XS}}$	7.40 ± 0.13^{r}	6.599 ± 0.051^{r}	5.30 ± 0.33^{r}
$Q_{\mathrm{W}}^{\mathrm{CA}}$	1.862 ± 0.079^{r}	1.833 ± 0.034^{r}	1.67 ± 0.29^{r}
$Q_{\mathrm{W}}^{\mathrm{PF-B}}$	4.53 ± 0.62^{r}	4.03 ± 0.24^{r}	2.7 ± 1.6^{r}
$Q_{\mathrm{W}}^{\mathrm{PF-N}}$	18.85 ± 0.61^{r}	16.77 ± 0.24^{r}	12.8 ± 1.5^{r}
$Q_{\mathrm{W}}^{\mathrm{PF-W}}$	0.65 ± 0.62^{r}	0.58 ± 0.24^{r}	0.0 ± 1.6^{r}
$Q_{\mathrm{W}}^{\mathrm{VC}}$	0.3590 ± 0.0055^{r}	0.6107 ± 0.0044^{r}	0.754 ± 0.046^{r}
$Q_{\mathrm{W}}^{\mathrm{XS}}$	-36.33 ± 0.63^{r}	-32.16 ± 0.25^{r}	-25.7 ± 1.6^{r}

^{r} Uncertainty determined from replicate experiments.

^{s} Uncertainty estimated from linear error propagation.

Table S19: Loadings (units of molec/uc) at Different Concentrations (units of g/L) of B/W onto MFI-F at 323 K.

$C_{B,eq}$	0.0406 ± 0.0035^r	3.89 ± 0.37^r	4.17 ± 0.39^r	4.49 ± 0.19^s	11.6 ± 1.9^s	15.85 ± 0.75^s	698 ± 20^s
Q_B^{CA}	0.0939 ± 0.0015^r	0.636 ± 0.092^r	2.300 ± 0.074^r	5.4 ± 1.1^s	7.3 ± 1.9^s	8.26 ± 0.28^s	9 ± 15^s
Q_B^{NS}	0.0939 ± 0.0015^r	0.636 ± 0.092^r	2.298 ± 0.075^r	5.4 ± 1.1^s	7.3 ± 1.9^s	8.26 ± 0.28^s	9 ± 21^s
Q_B^{PF-B}	0.0942 ± 0.0015^r	0.667 ± 0.089^r	2.325 ± 0.072^r	5.4 ± 1.1^s	7.3 ± 1.9^s	8.27 ± 0.27^s	8.7 ± 6.4^s
Q_B^{PF-N}	0.0943 ± 0.0014^r	0.679 ± 0.088^r	2.338 ± 0.071^r	5.5 ± 1.1^s	7.4 ± 1.9^s	8.31 ± 0.27^s	10.8 ± 6.4^s
Q_B^{PF-W}	0.0942 ± 0.0015^r	0.664 ± 0.089^r	2.322 ± 0.072^r	5.4 ± 1.1^s	7.3 ± 1.9^s	8.25 ± 0.27^s	8.1 ± 6.5^s
Q_B^{VC}	0.0939 ± 0.0015^r	0.636 ± 0.092^r	2.298 ± 0.075^r	5.4 ± 1.1^s	7.3 ± 1.9^s	8.26 ± 0.28^s	9 ± 21^s
Q_B^{XS}	0.0939 ± 0.0015^r	0.633 ± 0.092^r	2.289 ± 0.075^r	5.4 ± 1.1^s	7.2 ± 1.9^s	8.13 ± 0.28^s	2.6 ± 6.6^s
Q_W^{CA}	0.4120 ± 0.0014^r	0.909 ± 0.079^r	2.063 ± 0.039^r	2.72 ± 0.12^s	2.15 ± 0.94^s	1.61 ± 0.19^s	1 ± 13^s
Q_W^{PF-B}	43.2156 ± 0.0072^r	40.37 ± 0.44^r	32.16 ± 0.36^r	16.7 ± 5.4^s	7.3 ± 9.4^s	2.7 ± 1.4^s	0 ± 32^s
Q_W^{PF-N}	58.4089 ± 0.0071^r	55.51 ± 0.43^r	47.29 ± 0.35^r	31.8 ± 5.4^s	22.3 ± 9.4^s	17.7 ± 1.3^s	5 ± 32^s
Q_W^{PF-W}	39.1007 ± 0.0072^r	36.28 ± 0.44^r	28.06 ± 0.36^r	12.6 ± 5.4^s	3.2 ± 9.4^s	-1.3 ± 1.4^s	-1 ± 32^s
Q_W^{VC}	0.001061 ± 0.000017^r	0.0089 ± 0.0012^r	0.03663 ± 0.00094^r	0.105 ± 0.027^s	0.183 ± 0.060^s	0.2301 ± 0.0082^s	0.39 ± 0.96^s
Q_W^{XS}	-0.4641 ± 0.0073^r	-3.13 ± 0.45^r	-11.31 ± 0.37^r	-26.7 ± 5.4^s	-35.7 ± 9.4^s	-40.0 ± 1.4^s	-13 ± 33^s

^{r} Uncertainty determined from replicate experiments.

^{s} Uncertainty estimated from linear error propagation.

Table S20: Loadings (units of molec/uc) at Different Concentrations (units of g/L) of P/W onto MFI-OH at 323 K.

$C_{P,eq}$	0.0247 ± 0.0022^s	0.152 ± 0.013^r	0.182 ± 0.012^r	0.300 ± 0.022^s	0.471 ± 0.054^s	9.40 ± 0.10^s
Q_P^{CA}	0.00006 ± 0.00069^s	0.0086 ± 0.0030^r	2.5892 ± 0.0082^r	4.23 ± 0.11^s	6.39 ± 0.16^s	6.81 ± 0.22^s
Q_P^{NS}	0.00006 ± 0.00069^s	0.0086 ± 0.0030^r	2.5891 ± 0.0082^r	4.23 ± 0.11^s	6.39 ± 0.16^s	6.81 ± 0.22^s
Q_P^{PF-N}	0.00031 ± 0.00068^s	0.0102 ± 0.0028^r	2.5905 ± 0.0082^r	4.23 ± 0.11^s	6.39 ± 0.16^s	6.84 ± 0.22^s
Q_P^{PF-P}	0.00026 ± 0.00068^s	0.0098 ± 0.0028^r	2.5901 ± 0.0082^r	4.23 ± 0.11^s	6.39 ± 0.16^s	6.82 ± 0.22^s
Q_P^{PF-W}	0.00023 ± 0.00068^s	0.0096 ± 0.0029^r	2.5899 ± 0.0082^r	4.23 ± 0.11^s	6.39 ± 0.16^s	6.81 ± 0.22^s
Q_P^{VC}	0.00006 ± 0.00069^s	0.0086 ± 0.0030^r	2.5891 ± 0.0082^r	4.23 ± 0.11^s	6.39 ± 0.16^s	6.81 ± 0.22^s
Q_P^{XS}	0.00006 ± 0.00069^s	0.0086 ± 0.0030^r	2.5886 ± 0.0082^r	4.23 ± 0.11^s	6.39 ± 0.16^s	6.75 ± 0.22^s
Q_W^{CA}	0.31998 ± 0.00063^s	0.3278 ± 0.0027^r	1.9660 ± 0.0029^r	2.26486 ± 0.00062^s	1.779 ± 0.075^s	1.56 ± 0.12^s
Q_W^{PF-N}	58.8619 ± 0.0040^s	58.804 ± 0.017^r	43.630 ± 0.048^r	33.97 ± 0.64^s	21.29 ± 0.96^s	18.6 ± 1.3^s
Q_W^{PF-P}	46.8363 ± 0.0040^s	46.780 ± 0.017^r	31.606 ± 0.048^r	21.94 ± 0.64^s	9.27 ± 0.96^s	6.7 ± 1.3^s
Q_W^{PF-W}	39.5576 ± 0.0040^s	39.502 ± 0.017^r	24.329 ± 0.048^r	14.67 ± 0.64^s	1.99 ± 0.96^s	-0.5 ± 1.3^s
Q_W^{VC}	$[(0.6 \pm 7.9) \times 10^{-5}]^s$	0.00098 ± 0.00034^r	0.29477 ± 0.00094^r	0.482 ± 0.012^s	0.727 ± 0.019^s	0.776 ± 0.026^s
Q_W^{XS}	-0.0003 ± 0.0040^s	-0.050 ± 0.017^r	-14.928 ± 0.047^r	-24.40 ± 0.62^s	-36.82 ± 0.94^s	-38.9 ± 1.3^s
$C_{P,eq}$	21.6 ± 1.3^s	47.2 ± 3.5^s	140.5 ± 2.4^s	467.6 ± 1.7^r	564.9 ± 1.3^r	623.20 ± 0.92^r
Q_P^{CA}	6.53 ± 0.41^s	7.45 ± 0.89^s	7.3 ± 1.2^s	7.14 ± 0.63^r	7.58 ± 0.54^r	7.35 ± 0.45^r
Q_P^{NS}	6.52 ± 0.42^s	7.44 ± 0.90^s	7.3 ± 1.2^s	6.93 ± 0.69^r	7.33 ± 0.63^r	6.99 ± 0.54^r
Q_P^{PF-N}	6.60 ± 0.40^s	7.57 ± 0.85^s	7.7 ± 1.0^s	8.40 ± 0.36^r	8.87 ± 0.26^r	8.90 ± 0.20^r
Q_P^{PF-P}	6.55 ± 0.41^s	7.47 ± 0.85^s	7.4 ± 1.0^s	7.43 ± 0.36^r	7.70 ± 0.27^r	7.61 ± 0.20^r
Q_P^{PF-W}	6.53 ± 0.41^s	7.41 ± 0.86^s	7.2 ± 1.0^s	6.84 ± 0.36^r	6.98 ± 0.27^r	6.82 ± 0.20^r
Q_P^{VC}	6.53 ± 0.42^s	7.45 ± 0.90^s	7.3 ± 1.2^s	7.06 ± 0.71^r	7.53 ± 0.64^r	7.23 ± 0.56^r
Q_P^{XS}	6.38 ± 0.41^s	7.09 ± 0.88^s	6.3 ± 1.0^s	3.66 ± 0.38^r	3.15 ± 0.28^r	2.60 ± 0.21^r
Q_W^{CA}	1.71 ± 0.20^s	1.17 ± 0.61^s	1.24 ± 0.78^s	1.35 ± 0.41^r	1.06 ± 0.40^r	1.23 ± 0.30^r
Q_W^{PF-N}	20.1 ± 2.4^s	14.4 ± 5.0^s	13.6 ± 6.0^s	9.5 ± 2.1^r	6.7 ± 1.6^r	6.5 ± 1.2^r
Q_W^{PF-P}	8.3 ± 2.4^s	2.9 ± 5.0^s	3.3 ± 6.0^s	3.2 ± 2.1^r	1.6 ± 1.6^r	2.1 ± 1.2^r
Q_W^{PF-W}	1.2 ± 2.4^s	-4.0 ± 5.0^s	-2.9 ± 6.1^s	-0.6 ± 2.1^r	-1.5 ± 1.6^r	-0.6 ± 1.2^r
Q_W^{VC}	0.743 ± 0.047^s	0.85 ± 0.10^s	0.83 ± 0.14^s	0.804 ± 0.080^r	0.857 ± 0.073^r	0.823 ± 0.064^r
Q_W^{XS}	-36.8 ± 2.4^s	-40.9 ± 5.1^s	-36.2 ± 6.0^s	-21.1 ± 2.2^r	-18.2 ± 1.6^r	-15.0 ± 1.2^r

^{r} Uncertainty determined from replicate experiments.

^{s} Uncertainty estimated from linear error propagation.

Table S21: Loadings (units of molec/uc) at Different Concentrations (units of g/L) of P/W onto MFI-F at 323 K.

$C_{\mathrm{P,eq}}$	0.073 ± 0.034^{r}	0.108 ± 0.012^{r}	0.145 ± 0.021^{r}	0.24 ± 0.16^{s}	56.8 ± 5.2^{r}	326.4 ± 3.9^{r}	594.0 ± 2.0^{r}
$Q_{\mathrm{P}}^{\mathrm{CA}}$	0.0661 ± 0.0073^{r}	1.2944 ± 0.0081^{r}	2.745 ± 0.016^{r}	5.669 ± 0.075^{s}	8.0 ± 1.2^{r}	7.9 ± 1.2^{r}	8.19 ± 0.87^{r}
$Q_{\mathrm{P}}^{\mathrm{NS}}$	0.0661 ± 0.0073^{r}	1.2944 ± 0.0081^{r}	2.745 ± 0.016^{r}	5.668 ± 0.075^{s}	8.0 ± 1.2^{r}	7.8 ± 1.2^{r}	8.0 ± 1.1^{r}
$Q_{\mathrm{P}}^{\mathrm{PF-N}}$	0.0668 ± 0.0070^{r}	1.2953 ± 0.0080^{r}	2.746 ± 0.016^{r}	5.670 ± 0.075^{s}	8.1 ± 1.1^{r}	8.53 ± 0.82^{r}	9.23 ± 0.42^{r}
$Q_{\mathrm{P}}^{\mathrm{PF-P}}$	0.0667 ± 0.0070^{r}	1.2951 ± 0.0080^{r}	2.746 ± 0.016^{r}	5.669 ± 0.075^{s}	8.0 ± 1.1^{r}	7.85 ± 0.83^{r}	8.00 ± 0.42^{r}
$Q_{\mathrm{P}}^{\mathrm{PF-W}}$	0.0666 ± 0.0071^{r}	1.2950 ± 0.0080^{r}	2.746 ± 0.016^{r}	5.669 ± 0.075^{s}	7.9 ± 1.1^{r}	7.43 ± 0.84^{r}	7.25 ± 0.42^{r}
$Q_{\mathrm{P}}^{\mathrm{VC}}$	0.0661 ± 0.0073^{r}	1.2944 ± 0.0081^{r}	2.745 ± 0.016^{r}	5.669 ± 0.075^{s}	8.0 ± 1.2^{r}	7.9 ± 1.3^{r}	8.3 ± 1.1^{r}
$Q_{\mathrm{P}}^{\mathrm{XS}}$	0.0661 ± 0.0073^{r}	1.2942 ± 0.0081^{r}	2.745 ± 0.016^{r}	5.667 ± 0.075^{s}	7.5 ± 1.1^{r}	5.22 ± 0.87^{r}	3.23 ± 0.44^{r}
$Q_{\mathrm{W}}^{\mathrm{CA}}$	0.3798 ± 0.0066^{r}	1.3226 ± 0.0051^{r}	2.0192 ± 0.0053^{r}	2.052 ± 0.023^{s}	0.70 ± 0.93^{r}	0.81 ± 0.90^{r}	0.56 ± 0.74^{r}
$Q_{\mathrm{W}}^{\mathrm{PF-N}}$	58.471 ± 0.041^{r}	51.246 ± 0.047^{r}	42.715 ± 0.095^{r}	25.52 ± 0.44^{s}	11.2 ± 6.4^{r}	8.7 ± 4.8^{r}	4.6 ± 2.5^{r}
$Q_{\mathrm{W}}^{\mathrm{PF-P}}$	46.446 ± 0.041^{r}	39.222 ± 0.047^{r}	30.691 ± 0.095^{r}	13.50 ± 0.44^{s}	-0.1 ± 6.5^{r}	0.7 ± 4.9^{r}	-0.2 ± 2.5^{r}
$Q_{\mathrm{W}}^{\mathrm{PF-W}}$	39.167 ± 0.042^{r}	31.944 ± 0.047^{r}	23.413 ± 0.095^{r}	6.22 ± 0.44^{s}	-7.0 ± 6.5^{r}	-4.2 ± 4.9^{r}	-3.1 ± 2.5^{r}
$Q_{\mathrm{W}}^{\mathrm{VC}}$	0.00752 ± 0.00083^{r}	0.14737 ± 0.00092^{r}	0.3125 ± 0.0019^{r}	0.6454 ± 0.0085^{s}	0.91 ± 0.13^{r}	0.89 ± 0.14^{r}	0.94 ± 0.12^{r}
$Q_{\mathrm{W}}^{\mathrm{XS}}$	-0.381 ± 0.042^{r}	-7.464 ± 0.047^{r}	-15.828 ± 0.094^{r}	-32.68 ± 0.43^{s}	-43.4 ± 6.6^{r}	-30.1 ± 5.0^{r}	-18.6 ± 2.6^{r}

^{r} Uncertainty determined from replicate experiments.

^{s} Uncertainty estimated from linear error propagation.

Table S22: Loadings (units of molec/uc) at Different Concentrations (units of g/L) of E/W onto MFI-F at 323 K.

$C_{\mathrm{E,eq}}$	0.13 ± 0.11^{s}	1.73 ± 0.65^{s}	4.180 ± 0.048^{s}	17.7 ± 1.7^{s}	67 ± 12^{s}	110.4 ± 1.3^{s}	430.8 ± 1.3^{s}
$Q_{\mathrm{E}}^{\mathrm{CA}}$	0.245 ± 0.059^{s}	2.14 ± 0.38^{s}	4.26 ± 0.60^{s}	11.6 ± 1.1^{s}	13.0 ± 6.5^{s}	11.6 ± 1.9^{s}	11.6 ± 1.6^{s}
$Q_{\mathrm{E}}^{\mathrm{NS}}$	0.245 ± 0.059^{s}	2.14 ± 0.38^{s}	4.26 ± 0.60^{s}	11.6 ± 1.1^{s}	13.0 ± 6.6^{s}	11.6 ± 1.9^{s}	11.3 ± 1.7^{s}
$Q_{\mathrm{E}}^{\mathrm{PF-E}}$	0.247 ± 0.057^{s}	2.17 ± 0.37^{s}	4.31 ± 0.60^{s}	11.6 ± 1.1^{s}	13.0 ± 6.0^{s}	11.8 ± 1.7^{s}	12.38 ± 0.77^{s}
$Q_{\mathrm{E}}^{\mathrm{PF-N}}$	0.248 ± 0.057^{s}	2.18 ± 0.37^{s}	4.33 ± 0.60^{s}	11.7 ± 1.1^{s}	13.4 ± 5.9^{s}	12.5 ± 1.7^{s}	14.83 ± 0.77^{s}
$Q_{\mathrm{E}}^{\mathrm{PF-W}}$	0.247 ± 0.058^{s}	2.16 ± 0.37^{s}	4.30 ± 0.60^{s}	11.6 ± 1.1^{s}	12.9 ± 6.0^{s}	11.6 ± 1.7^{s}	11.65 ± 0.77^{s}
$Q_{\mathrm{E}}^{\mathrm{VC}}$	0.245 ± 0.059^{s}	2.14 ± 0.38^{s}	4.26 ± 0.60^{s}	11.6 ± 1.1^{s}	13.1 ± 6.6^{s}	11.7 ± 2.0^{s}	11.7 ± 1.8^{s}
$Q_{\mathrm{E}}^{\mathrm{XS}}$	0.245 ± 0.059^{s}	2.14 ± 0.38^{s}	4.24 ± 0.60^{s}	11.3 ± 1.1^{s}	11.9 ± 6.2^{s}	10.0 ± 1.7^{s}	5.10 ± 0.78^{s}
$Q_{\mathrm{W}}^{\mathrm{CA}}$	0.402 ± 0.020^{s}	0.935 ± 0.088^{s}	1.307 ± 0.072^{s}	0.78 ± 0.30^{s}	0.4 ± 2.2^{s}	0.77 ± 0.51^{s}	0.78 ± 0.41^{s}
$Q_{\mathrm{W}}^{\mathrm{PF-E}}$	43.14 ± 0.19^{s}	36.8 ± 1.2^{s}	29.7 ± 2.0^{s}	5.4 ± 3.7^{s}	1 ± 20^{s}	4.8 ± 5.5^{s}	3.0 ± 2.6^{s}
$Q_{\mathrm{W}}^{\mathrm{PF-N}}$	58.00 ± 0.19^{s}	51.6 ± 1.2^{s}	44.5 ± 2.0^{s}	20.0 ± 3.7^{s}	14 ± 20^{s}	17.5 ± 5.5^{s}	9.7 ± 2.5^{s}
$Q_{\mathrm{W}}^{\mathrm{PF-W}}$	38.71 ± 0.19^{s}	32.4 ± 1.2^{s}	25.3 ± 2.0^{s}	1.1 ± 3.7^{s}	-3 ± 20^{s}	1.0 ± 5.5^{s}	1.0 ± 2.6^{s}
$Q_{\mathrm{W}}^{\mathrm{VC}}$	0.056 ± 0.014^{s}	0.496 ± 0.088^{s}	1.00 ± 0.14^{s}	2.89 ± 0.28^{s}	3.5 ± 1.8^{s}	3.24 ± 0.54^{s}	1.08 ± 0.17^{s}
$Q_{\mathrm{W}}^{\mathrm{XS}}$	-0.75 ± 0.18^{s}	-6.6 ± 1.2^{s}	-13.0 ± 1.8^{s}	-34.7 ± 3.5^{s}	-36 ± 19^{s}	-30.5 ± 5.1^{s}	-17.1 ± 2.6^{s}

^{s} Uncertainty estimated from linear error propagation.

Table S23: Loadings (units of molec/uc) at Different Concentrations (units of g/L) of P/E onto MFI-OH at 323 K.

$C_{\mathrm{P,eq}}$	9.04 ± 0.40^{r}	29.14 ± 0.23^{s}	30.11 ± 0.20^{s}	44.75 ± 0.77^{r}	53.84 ± 0.42^{r}	87.04 ± 0.20^{s}	97.78 ± 0.20^{s}
$Q_{\mathrm{P}}^{\mathrm{CA}}$	0.66 ± 0.13^{r}	0.67 ± 0.15^{s}	0.65 ± 0.15^{s}	1.56 ± 0.17^{r}	0.989 ± 0.088^{r}	1.49 ± 0.19^{s}	1.95 ± 0.21^{s}
$Q_{\mathrm{P}}^{\mathrm{NS}}$	0.59 ± 0.13^{r}	0.46 ± 0.16^{s}	0.42 ± 0.15^{s}	1.26 ± 0.18^{r}	0.595 ± 0.096^{r}	0.88 ± 0.21^{s}	1.30 ± 0.23^{s}
$Q_{\mathrm{P}}^{\mathrm{PF-E}}$	0.66 ± 0.13^{r}	0.67 ± 0.15^{s}	0.64 ± 0.15^{s}	1.55 ± 0.17^{r}	0.977 ± 0.088^{r}	1.47 ± 0.19^{s}	1.92 ± 0.21^{s}
$Q_{\mathrm{P}}^{\mathrm{PF-N}}$	0.68 ± 0.12^{r}	0.74 ± 0.15^{s}	0.72 ± 0.15^{s}	1.66 ± 0.16^{r}	1.117 ± 0.087^{r}	1.70 ± 0.19^{s}	2.18 ± 0.21^{s}
$Q_{\mathrm{P}}^{\mathrm{PF-P}}$	0.66 ± 0.13^{r}	0.68 ± 0.15^{s}	0.65 ± 0.15^{s}	1.57 ± 0.16^{r}	1.003 ± 0.088^{r}	1.52 ± 0.19^{s}	1.97 ± 0.21^{s}
$Q_{\mathrm{P}}^{\mathrm{VC}}$	0.59 ± 0.13^{r}	0.46 ± 0.16^{s}	0.42 ± 0.15^{s}	1.26 ± 0.18^{r}	0.595 ± 0.096^{r}	0.88 ± 0.21^{s}	1.30 ± 0.23^{s}
$Q_{\mathrm{P}}^{\mathrm{XS}}$	0.59 ± 0.13^{r}	0.44 ± 0.15^{s}	0.41 ± 0.15^{s}	1.20 ± 0.17^{r}	0.562 ± 0.091^{r}	0.80 ± 0.19^{s}	1.17 ± 0.21^{s}
$Q_{\mathrm{E}}^{\mathrm{CA}}$	12.47 ± 0.21^{r}	12.45 ± 0.25^{s}	12.50 ± 0.25^{s}	10.96 ± 0.28^{r}	11.92 ± 0.15^{r}	11.07 ± 0.32^{s}	10.30 ± 0.36^{s}
$Q_{\mathrm{E}}^{\mathrm{PF-E}}$	12.11 ± 0.22^{r}	12.09 ± 0.27^{s}	12.14 ± 0.26^{s}	10.53 ± 0.29^{r}	11.54 ± 0.16^{r}	10.66 ± 0.33^{s}	9.86 ± 0.37^{s}
$Q_{\mathrm{E}}^{\mathrm{PF-N}}$	16.55 ± 0.22^{r}	16.45 ± 0.27^{s}	16.49 ± 0.26^{s}	14.82 ± 0.29^{r}	15.78 ± 0.15^{r}	14.75 ± 0.33^{s}	13.90 ± 0.37^{s}
$Q_{\mathrm{E}}^{\mathrm{PF-P}}$	12.96 ± 0.22^{r}	12.93 ± 0.27^{s}	12.97 ± 0.26^{s}	11.35 ± 0.29^{r}	12.35 ± 0.16^{r}	11.45 ± 0.33^{s}	10.63 ± 0.37^{s}
$Q_{\mathrm{E}}^{\mathrm{XS}}$	-1.04 ± 0.23^{r}	-0.79 ± 0.27^{s}	-0.72 ± 0.26^{s}	-2.13 ± 0.30^{r}	-1.00 ± 0.16^{r}	-1.42 ± 0.33^{s}	-2.08 ± 0.37^{s}
$C_{\mathrm{P,eq}}$	258.4 ± 1.8^{r}	338.4 ± 1.8^{r}	458.8 ± 1.8^{r}				
$Q_{\mathrm{P}}^{\mathrm{CA}}$	5.85 ± 0.44^{r}	6.72 ± 0.34^{r}	7.17 ± 0.39^{r}				
$Q_{\mathrm{P}}^{\mathrm{NS}}$	5.09 ± 0.60^{r}	6.03 ± 0.51^{r}	6.40 ± 0.72^{r}				
$Q_{\mathrm{P}}^{\mathrm{PF-E}}$	5.73 ± 0.44^{r}	6.54 ± 0.33^{r}	6.91 ± 0.38^{r}				
$Q_{\mathrm{P}}^{\mathrm{PF-N}}$	6.40 ± 0.43^{r}	7.42 ± 0.33^{r}	8.11 ± 0.37^{r}				
$Q_{\mathrm{P}}^{\mathrm{PF-P}}$	5.86 ± 0.44^{r}	6.71 ± 0.33^{r}	7.14 ± 0.38^{r}				
$Q_{\mathrm{P}}^{\mathrm{VC}}$	5.09 ± 0.60^{r}	6.03 ± 0.51^{r}	6.40 ± 0.72^{r}				
$Q_{\mathrm{P}}^{\mathrm{XS}}$	3.74 ± 0.45^{r}	3.93 ± 0.35^{r}	3.38 ± 0.39^{r}				
$Q_{\mathrm{E}}^{\mathrm{CA}}$	3.72 ± 0.75^{r}	2.27 ± 0.57^{r}	1.51 ± 0.65^{r}				
$Q_{\mathrm{E}}^{\mathrm{PF-E}}$	3.11 ± 0.78^{r}	1.67 ± 0.59^{r}	1.01 ± 0.67^{r}				
$Q_{\mathrm{E}}^{\mathrm{PF-N}}$	6.40 ± 0.77^{r}	4.60 ± 0.58^{r}	3.38 ± 0.66^{r}				
$Q_{\mathrm{E}}^{\mathrm{PF-P}}$	3.74 ± 0.78^{r}	2.23 ± 0.59^{r}	1.46 ± 0.67^{r}				
$Q_{\mathrm{E}}^{\mathrm{XS}}$	-6.64 ± 0.80^{r}	-6.98 ± 0.61^{r}	-6.00 ± 0.69^{r}				

^{r} Uncertainty determined from replicate experiments.

^{s} Uncertainty estimated from linear error propagation.

Table S24: Loadings (units of molec/uc) at Different Concentrations (units of g/L) of P/E onto MFI-F at 323 K.

$C_{\mathrm{P,eq}}$	7.6 ± 1.5^{r}	29.28 ± 0.16^{r}	49.5 ± 1.5^{r}	64.773801 ± 0^{s}	91.3 ± 3.3^{s}	171 ± 13^{s}	254.72 ± 0.68^{r}
$Q_{\mathrm{P}}^{\mathrm{CA}}$	0.37 ± 0.32^{r}	0.270 ± 0.034^{r}	0.81 ± 0.32^{r}	1.12 ± 0.64^{s}	1.3 ± 2.1^{s}	2.9 ± 4.4^{s}	4.99 ± 0.15^{r}
$Q_{\mathrm{P}}^{\mathrm{NS}}$	0.32 ± 0.34^{r}	0.040 ± 0.037^{r}	0.44 ± 0.35^{r}	0.65 ± 0.68^{s}	0.7 ± 2.3^{s}	1.9 ± 5.3^{s}	3.95 ± 0.20^{r}
$Q_{\mathrm{P}}^{\mathrm{PF-E}}$	0.37 ± 0.32^{r}	0.264 ± 0.034^{r}	0.80 ± 0.32^{r}	1.10 ± 0.63^{s}	1.3 ± 2.1^{s}	2.9 ± 4.3^{s}	4.87 ± 0.15^{r}
$Q_{\mathrm{P}}^{\mathrm{PF-N}}$	0.39 ± 0.32^{r}	0.340 ± 0.034^{r}	0.93 ± 0.32^{r}	1.27 ± 0.63^{s}	1.5 ± 2.1^{s}	3.3 ± 4.3^{s}	5.54 ± 0.15^{r}
$Q_{\mathrm{P}}^{\mathrm{PF-P}}$	0.38 ± 0.32^{r}	0.278 ± 0.034^{r}	0.82 ± 0.32^{r}	1.14 ± 0.63^{s}	1.3 ± 2.1^{s}	3.0 ± 4.3^{s}	5.00 ± 0.15^{r}
$Q_{\mathrm{P}}^{\mathrm{VC}}$	0.32 ± 0.34^{r}	0.040 ± 0.037^{r}	0.44 ± 0.35^{r}	0.65 ± 0.68^{s}	0.7 ± 2.3^{s}	1.9 ± 5.3^{s}	3.95 ± 0.20^{r}
$Q_{\mathrm{P}}^{\mathrm{XS}}$	0.31 ± 0.33^{r}	0.039 ± 0.036^{r}	0.42 ± 0.33^{r}	0.61 ± 0.63^{s}	0.6 ± 2.1^{s}	1.6 ± 4.4^{s}	2.91 ± 0.15^{r}
$Q_{\mathrm{E}}^{\mathrm{CA}}$	12.95 ± 0.54^{r}	13.130 ± 0.058^{r}	12.22 ± 0.54^{r}	11.7 ± 1.1^{s}	11.4 ± 3.5^{s}	8.6 ± 7.4^{s}	5.18 ± 0.25^{r}
$Q_{\mathrm{E}}^{\mathrm{PF-E}}$	12.61 ± 0.57^{r}	12.807 ± 0.061^{r}	11.86 ± 0.57^{r}	11.3 ± 1.1^{s}	11.0 ± 3.7^{s}	8.2 ± 7.7^{s}	4.62 ± 0.26^{r}
$Q_{\mathrm{E}}^{\mathrm{PF-N}}$	17.07 ± 0.57^{r}	17.161 ± 0.060^{r}	16.12 ± 0.56^{r}	15.5 ± 1.1^{s}	15.0 ± 3.7^{s}	11.9 ± 7.7^{s}	7.94 ± 0.26^{r}
$Q_{\mathrm{E}}^{\mathrm{PF-P}}$	13.47 ± 0.57^{r}	13.641 ± 0.061^{r}	12.68 ± 0.57^{r}	12.1 ± 1.1^{s}	11.8 ± 3.7^{s}	8.9 ± 7.7^{s}	5.26 ± 0.26^{r}
$Q_{\mathrm{E}}^{\mathrm{XS}}$	-0.56 ± 0.59^{r}	-0.069 ± 0.063^{r}	-0.74 ± 0.59^{r}	-1.1 ± 1.1^{s}	-1.1 ± 3.7^{s}	-2.8 ± 7.8^{s}	-5.17 ± 0.27^{r}
$C_{\mathrm{P,eq}}$	349.2 ± 1.3^{r}	480.09 ± 0.75^{r}					
$Q_{\mathrm{P}}^{\mathrm{CA}}$	6.37 ± 0.30^{r}	7.34 ± 0.16^{r}					
$Q_{\mathrm{P}}^{\mathrm{NS}}$	5.47 ± 0.46^{r}	6.67 ± 0.31^{r}					
$Q_{\mathrm{P}}^{\mathrm{PF-E}}$	6.19 ± 0.29^{r}	7.07 ± 0.16^{r}					
$Q_{\mathrm{P}}^{\mathrm{PF-N}}$	7.10 ± 0.29^{r}	8.32 ± 0.16^{r}					
$Q_{\mathrm{P}}^{\mathrm{PF-P}}$	6.37 ± 0.29^{r}	7.31 ± 0.16^{r}					
$Q_{\mathrm{P}}^{\mathrm{VC}}$	5.47 ± 0.46^{r}	6.67 ± 0.31^{r}					
$Q_{\mathrm{P}}^{\mathrm{XS}}$	3.51 ± 0.30^{r}	3.38 ± 0.16^{r}					
$Q_{\mathrm{E}}^{\mathrm{CA}}$	2.85 ± 0.50^{r}	1.22 ± 0.27^{r}					
$Q_{\mathrm{E}}^{\mathrm{PF-E}}$	2.28 ± 0.52^{r}	0.73 ± 0.28^{r}					
$Q_{\mathrm{E}}^{\mathrm{PF-N}}$	5.16 ± 0.51^{r}	3.00 ± 0.28^{r}					
$Q_{\mathrm{E}}^{\mathrm{PF-P}}$	2.83 ± 0.52^{r}	1.16 ± 0.28^{r}					
$Q_{\mathrm{E}}^{\mathrm{XS}}$	-6.22 ± 0.54^{r}	-5.99 ± 0.29^{r}					

^{r} Uncertainty determined from replicate experiments.

^{s} Uncertainty estimated from linear error propagation.

References

(S1) Hnědkovský, L.; Cibulka, I. Partial Molar Volumes and Partial Molar Isentropic Compressions of Selected Alkane-α,ω-diols at Infinite Dilution in Water at Temperatures T = (278 to 318) K and Atmospheric Pressure. *J. Chem. Eng. Data* **2013**, *58*, 1724–1734.

(S2) Moosavi, M.; Rostami, A. A. Densities, Viscosities, Refractive Indices, and Excess Properties of Aqueous 1,2-Etanediol, 1,3-Propanediol, 1,4-Butanediol, and 1,5-Pentanediol Binary Mixtures. *J. Chem. Eng. Data* **2016**, *62*, 156–168.

(S3) Pires, R.; Costa, H.; Ferreira, A.; Fonseca, I. Viscosity and Density of Water + Ethyl Acetate + Ethanol Mixtures at 298.15 and 318.15 K and Atmospheric Pressure. *J. Chem. Eng. Data* **2007**, *52*, 1240–1245.

(S4) Trzpit, M.; Soulard, M.; Patarin, J.; Desbiens, N.; Cailliez, F.; Boutin, A.; Demachy, I.; Fuchs., A. H. The Effect of Local Defects on Water Adsorption in Silicalite-1 Zeolite: A Joint Experimental and Molecular Simulation Study. *Langmuir* **2007**, *23*, 10131–10139.

(S5) Bai, P.; Tsapatsis, M.; Siepmann, J. I. TraPPE-Zeo: Transferable Potentials for Phase Equilibria Force Field for All-Silica Zeolites. *J. Phys. Chem. C.* **2013**, *117*, 24375–24387.

(S6) Smith, B. D.; Srivastava, R. *Thermodynamics Data for Pure Compounds*; Elsevier: Amsterdam, 1986; p 284.

(S7) Takiguchi, Y.; Osada, O.; Uematsu, M. Thermodynamic Properties of $x\mathrm{C_2H_5OH}+(1-x)\mathrm{H_2O}$ in the Temperature Range From 320 K to 420 K at Pressures Up to 200 MPa. *J. Chem. Thermodynamics* **1996**, *28*, 1375–1385.

(S8) DeJaco, R. F.; Elyassi, B.; Dorneles de Mello, M.; Mittal, N.; Tsapatsis, M.; Siepmann, J. I. Understanding the Unique Sorption of Alkane-α,ω-Diols in Silicalite-1. *J. Chem. Phys.* **2018**, *149*, 072331.

(S9) Fegan, S. G.; Lowe, B. M. Sorption of Alkanediols by Silicalite-1. *J. Inclusion Phenom. Mol. Recognit. Chem.* **1989**, *7*, 461–464.

(S10) Kretschmer, C.; Wiebe, R. Liquid-Vapor Equilibrium of Ethanol–Toluene Solutions. *J. Am. Chem. Soc.* **1949**, *71*, 1793–1797.

(S11) Hyland, R.; Wexler, A. Formulations for the Thermodynamic Properties of the Saturated Phases of H_2O from 173.15 K to 473.15 K. *ASHRAE Trans. A* **1983**, *89*, 500–519.